ELSEVIER

Chemical Geology 129 (1996) 39–69

CHEMICAL GEOLOGY
INCLUDING
ISOTOPE GEOSCIENCE

Enriched Nd–Sr–Pb isotopic signatures in the Dovyren layered intrusion (eastern Siberia, Russia): evidence for source contamination by ancient upper-crustal material

Yu.V. Amelin [a,b,*], L.A. Neymark [a,c], E.Yu. Ritsk [a], A.A. Nemchin [a,d]

[a] *Institute of Precambrian Geology and Geochronology, Russian Academy of Science, Makarova emb. 2, St. Petersburg 199034, Russia*
[b] *Geochronology Laboratory, Royal Ontario Museum, 100 Queen's Park, Toronto, Ont. M5S 2C6, Canada*
[c] *U.S. Geological Survey, Box 25046, M.S. 963, Denver Federal Center, Denver, CO 80225, USA*
[d] *School of Applied Geology, Curtin University of Technology, GPO Box U 1987, Perth, W.A. 6001, Australia*

Received 1 June 1994; accepted 22 August 1995

Abstract

Major- and trace-element concentrations and Nd-, Sr- and Pb-isotopic ratios are reported for the Dovyren layered mafic–ultramafic intrusion in the northern Baikal region, eastern Siberia. Sm–Nd internal isochrons for an olivine gabbro from the layered series and a gabbronorite from a sill at the bottom of the Dovyren intrusion yield ages of 673 ± 22 and 707 ± 40 Ma, respectively. Initial isotopic ratios: $^{87}Sr/^{86}Sr$ (673) from 0.7101 to 0.7135, ε_{Nd}(673 Ma) from −16.3 to −14.1, $^{206}Pb/^{204}Pb$ from 16.80 to 17.14, $^{207}Pb/^{204}Pb$ from 15.477 to 15.501 and $^{208}Pb/^{204}Pb$ from 37.17 to 37.59, are similar to those of late Archean–early Proterozoic upper continental crust, but do not appear to be a result of wallrock assimilation in the magma chamber. These isotopic features, as well as high K, Rb and LREE and low Ti concentrations in the calculated composition of the Dovyren parental magma, may be explained by subduction of sediments derived from upper continental crust into depleted mantle and subsequent melting of the metasomatized peridotite.

1. Introduction

Isotopic studies of layered mafic–ultramafic intrusions provide valuable information on the processes of contamination of mafic magmas. Most models of interaction between mafic magma and crustal rocks were inferred from, or tested using isotopic data for layered intrusions. Models of bulk assimilation of crustal rocks or crust-derived melts were used in earlier studies (Gray et al., 1981; Zindler et al., 1981). A number of more sophisticated models were also applied to layered intrusions: combined assimilation and fractional crystallization, AFC (DePaolo, 1981) to the Kiglapait (Labrador, Canada) and Skærgaard (East Greenland) intrusions (DePaolo, 1985; Stewart and DePaolo, 1990); and refilling, tapping, fractionation, assimilation, RTFA (O'Hara, 1977) to the mafic complex in the Ivrea Zone, Western Alps, Italy (Voshage et al., 1990) and the Fozzano complex, Corsica, France (Poitrasson et al., 1994).

In addition, layered intrusions may acquire enriched isotopic and trace-element signatures because of contamination of a primary magma during ascent

* Corresponding author.

0009-2541/96/$15.00 © 1996 Elsevier Science B.V. All rights reserved
SSDI 0009-2541(95)00135-2

through continental crust (Huppert and Sparks, 1985). The unusual chemical and isotopic compositions may also be related to enrichment processes in their mantle sources. Isotopic studies of layered intrusions concentrated mostly on the contamination processes in magma chambers, but these processes and the pre-emplacement contamination and/or source enrichment are not mutually exclusive. In some cases, magma contamination and source enrichment can both contribute to the enriched isotopic and trace-element signatures, as was shown by Re–Os and Sm–Nd study of the Stillwater complex, Montana, U.S.A. (Lambert et al., 1989; Lambert et al., 1994). The diversity of proposed models for the genesis of layered intrusions probably reflects the multiplicity of processes operating during magma generation, ascent, emplacement and crystallization.

The Dovyren (also called Dovirensky or Yoko-Dovyren) mafic–ultramafic intrusion, northern Baikal region, eastern Siberia, is a large late Proterozoic layered intrusion, with well-preserved and almost completely exposed entire sequence of layered rocks and the lower marginal zone. The intrusion shows extensive evidence of crustal contamination, indicated by the presence of abundant metasedimentary xenoliths (Gurulev, 1965, Gurulev, 1983), and high and variable $\delta^{18}O$ and initial $^{87}Sr/^{86}Sr$ (I_{Sr}) (Yaroshevsky et al., 1980; Krivopliasov et al., 1984; Kislov et al., 1989). We therefore consider the Dovyren intrusion as an excellent example of an open magmatic system. In this paper we use elemental and Nd-, Sr- and Pb-isotopic data, and major- and trace-element concentrations to investigate the contamination processes that may ensue when a large mafic body is emplaced in the crust.

2. Geology of the Dovyren intrusion

The Dovyren intrusion is situated in the northern flank of the Riphean Olokit trough, within the long-lived, tectonically active Baikal fold area, near the

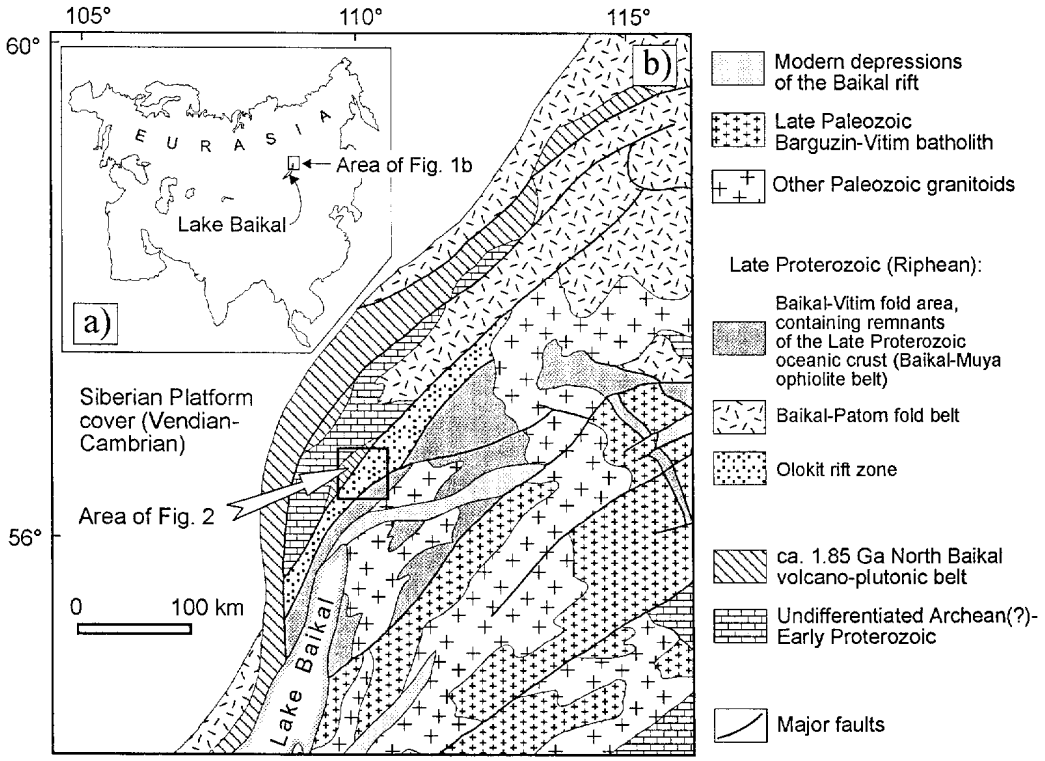

Fig. 1. a. Regional setting of the Baikal fold area.
b. Principal tectonic units of the Baikal fold area.

margin of the Siberian Platform (Salop, 1967; Neymark et al., 1991a, Neymark et al., 1991b). The tectonic structure of the Baikal fold area and the geological setting of the Dovyren intrusion are shown in Figs. 1 and 2, respectively. Within the Olokit trough, the intrusion forms the margin of the Ondoko paleo-uplift, separating two paleo-rifts (Fig. 2).

The Dovyren intrusion is a lopolith, concordant with the enclosing metasedimentary sequence. The body is ~ 26 km long and has a maximum stratigraphic thickness of 3.7 km. The present subvertical position of the intrusion and enclosing metasediments is the result of deformation during regional metamorphism at 550 Ma (Neymark et al., 1991b). The country rocks are high-alumina chloritoid-, quartz– sericite- and carbonaceous schists and quartz meta-sandstones containing layers of quartzites and dolomites. The host rocks are hornfelsed near the contacts with the Dovyren intrusion and accompanying mafic and ultramafic sills. Low-temperature regional metamorphism (chlorite–sericite subfacies of greenschist facies) affected the outer parts of the marginal zone of the intrusion, whereas the layered series and sills completely preserve their primary igneous mineral assemblages.

The internal structure of the Dovyren intrusion has been described by several workers (Gurulev, 1983; Yaroshevsky et al., 1983; Konnikov et al., 1988), and is shown in Fig. 3. The proposed schemes of petrologic subdivision of the intrusion are similar in the main features, but differ in interpretation of the lower marginal zone and of the uppermost gab-

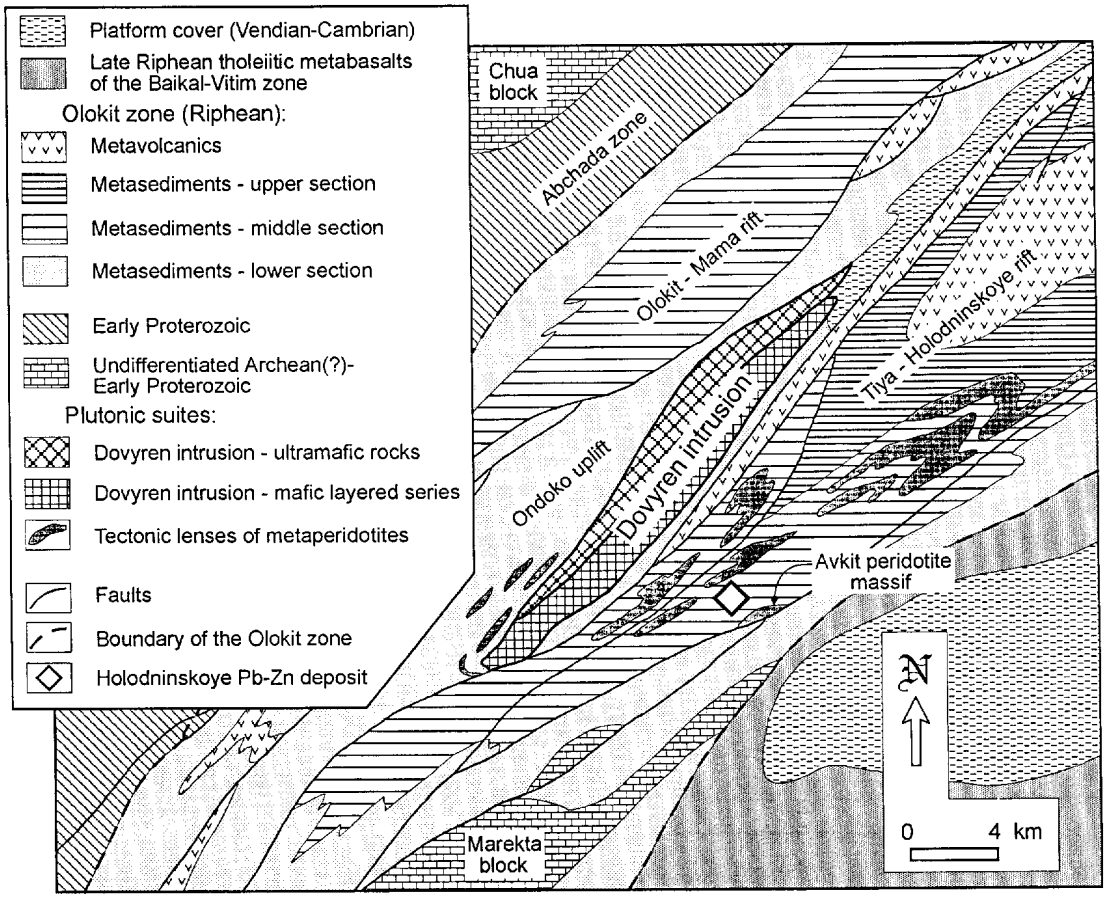

Fig. 2. Geological setting of the Dovyren layered intrusion in the Olokit rift zone of the Baikal fold area.

bronorite zone. The literal nomenclature of zones used in this paper (Fig. 4) is after Yaroshevsky et al. (1983) and Ionov et al. (1984a,b).

The lower marginal zone is graded from gabbroic harrisite to peridotite. The base of the lower marginal zone comprises quenched pyroxene–plagioclase aggregate in an olivine matrix that is as much as 2 m thick. The overlying plagioclase-bearing peridotite forms the remainder of the 150–200-m-thick lower marginal zone. Also included in the lower marginal zone is minor olivine gabbro and ophitic gabbronorite (Gurulev, 1983). Sills of plagioclase-bearing peridotite, gabbronorite, granophyre-bearing gabbro and diabase, similar in composition to the rocks of the lower marginal zone, are located within the metasedimentary rocks below the base of the Dovyren intrusion.

Above the lower marginal zone is a layered series that ranges in composition from dunite to gabbronorite. The layered series is subdivided into 5 zones (*A–E*), on the basis of cumulus mineral paragenesis (Yaroshevsky et al., 1983). The dunite zone (*A*) is an Ol and Ol + Cr-spinel cumulate. Intercumulus material is < 5% clinopyroxene, orthopyroxene and plagioclase. The lower part of zone *A*, ~ 150 m thick, is composed of plagioclase-bearing dunite with 5–10% Pl. Scattered partially digested dolomitic xenoliths (magnesian skarns) and gabbro-pegmatites occur in the upper part of the dunite zone (Fig. 4). Disseminated Cu–Ni-sulfide mineralization, com-

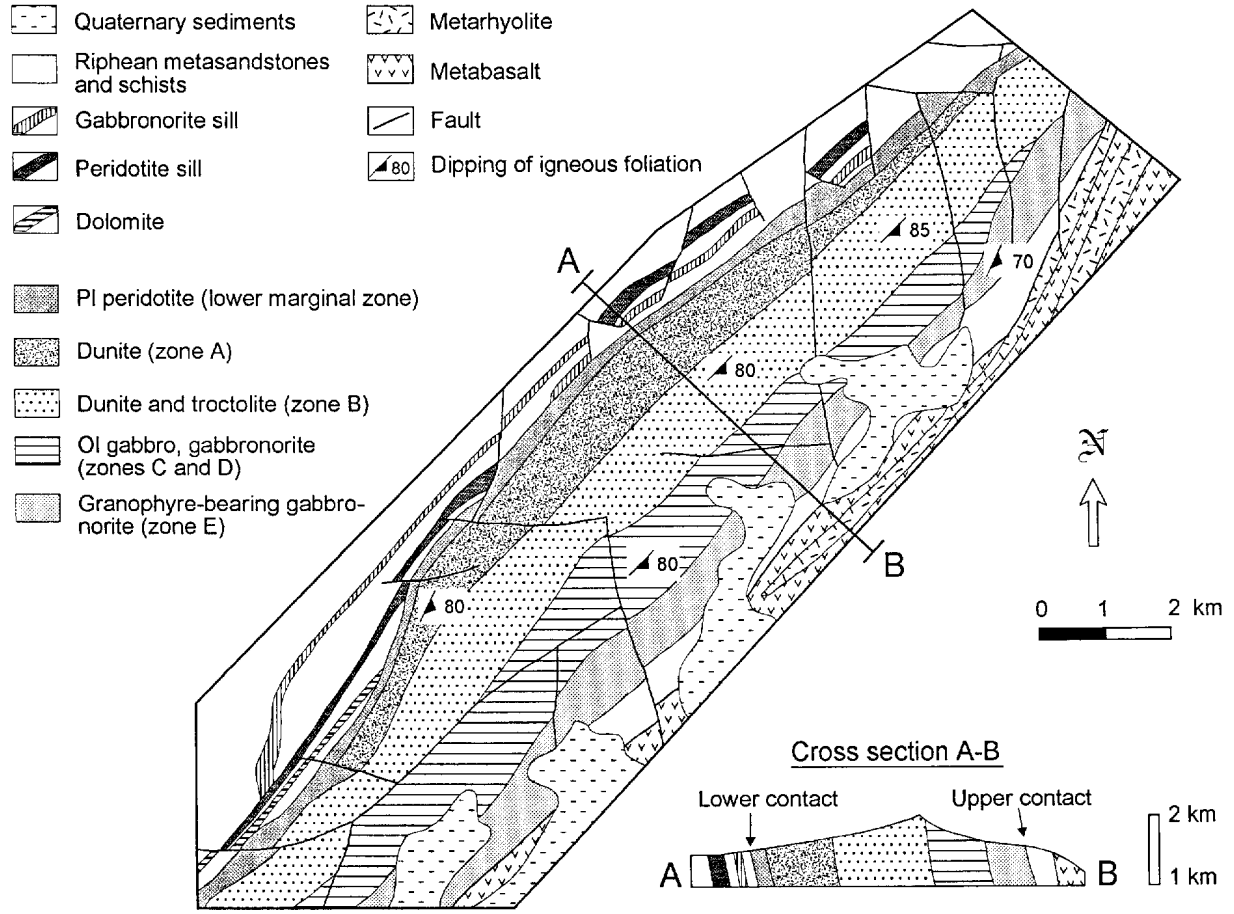

Fig. 3. Geological sketch map of the central part of the Dovyren intrusion, based on geological data of L.M. Baburin, V.A. Chabanenko, S.A. Gurulev, A.G. Krapivin, A.G. Stepin and the authors, and petrographic cross-sections of Gurulev (1983), Konnikov et al. (1988) and Yaroshevsky et al. (1983).

posed mostly of pyrrhotite and pentlandite, occurs in the lower marginal and dunite zones, and in ultramafic sills beneath the base of the intrusion (Konnikov et al., 1988, Konnikov et al., 1990; Papunen et al., 1992).

The troctolite zone (*B*) is composed of alternating layers of troctolite, dunite and plagioclase-bearing dunite. Cumulus minerals in the troctolites are olivine (70–85%) and plagioclase (10–25%), and small amounts of Cr-spinel; the main intercumulus mineral is clinopyroxene. Maximum thicknesses of zones *A* and *B* are 1050 and 1150 m, respectively. Zone *C* is composed of olivine gabbro (Ol + Cpx + Pl cumulate), and rare layers of troctolite. Zone *D* is also dominated by olivine gabbro, and, in addition, contains rocks with cumulus Opx: olivine-bearing gabbronorite (Ol + Cpx + Opx + Pl cumulate) and olivine-bearing norite (Ol + Opx + Pl cumulate). Olivine-free gabbronorite and norite are also present. Intercumulus mineral is clinopyroxene. Zone *E* is composed of gabbronorite and quartz- and granophyre-bearing gabbro and gabbronorite with sublayers of ophitic and olivine-bearing gabbro. Xenoliths of schists and meta-sandstones are common in

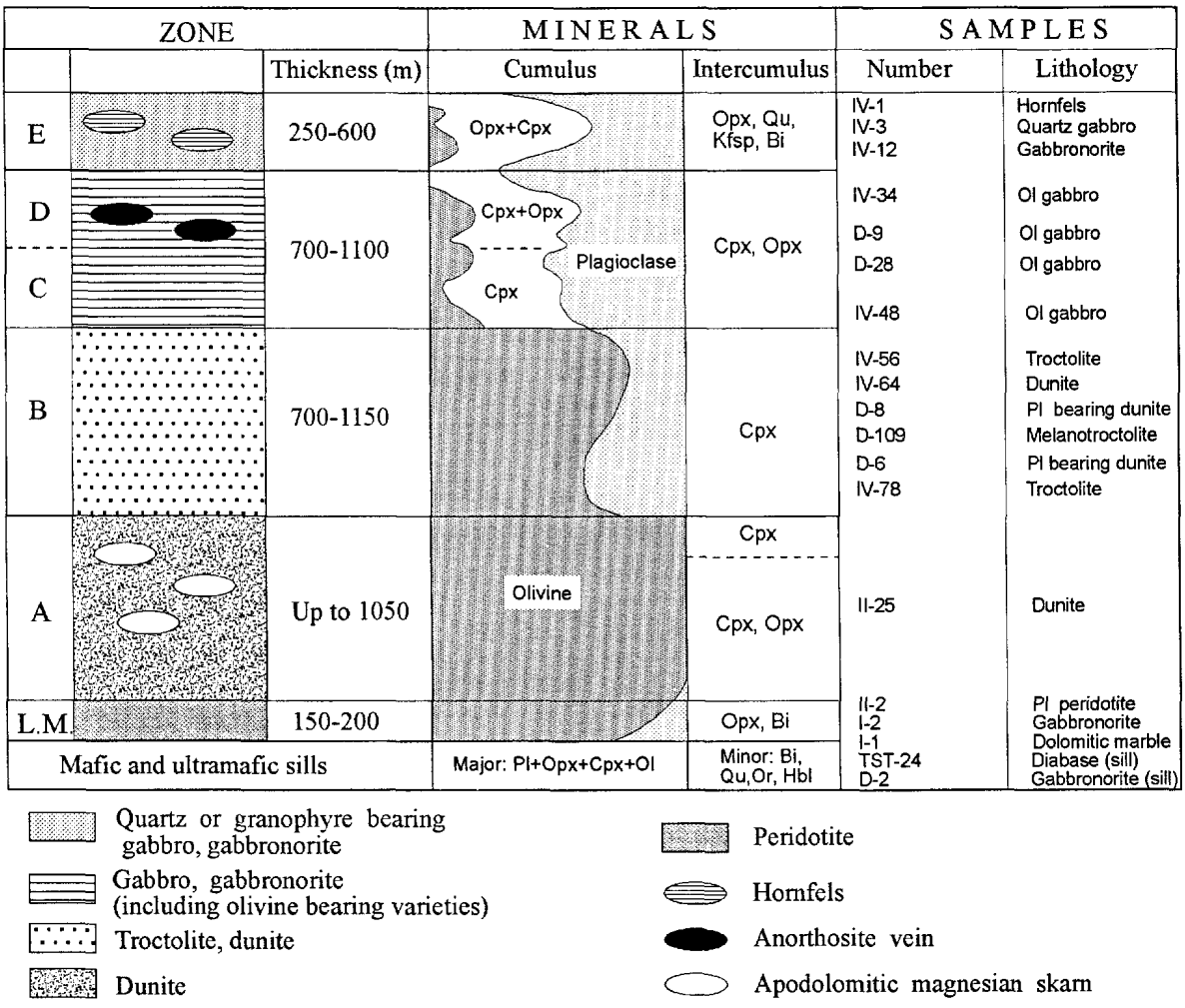

Fig. 4. Generalized cross-section of the Dovyren intrusion, showing stratigraphic positions of studied samples (from Gurulev, 1983; Konnikov et al., 1988; Yaroshevsky et al., 1983). Modal compositions are shown for predominant rock types and do not reflect lateral variations and the fine structure of the section (e.g., the presence of dunite and plagioclase-bearing dunite in zone *B*).

zone *E*. No marginal facies rocks are observed in the upper part of the Dovyren intrusion (Yaroshevsky et al., 1983). Thicknesses of zones *C–E* are shown in Fig. 4.

The age of the Dovyren massif is not well geochronologically constrained. It was first dated by Gerling et al. (1962) using the K–Ar method on biotite at 730–780 Ma. Kislov et al. (1989) obtained a Rb–Sr whole-rock age of 739 ± 55 Ma with initial $^{87}Sr/^{86}Sr = 0.7113 \pm 0.0002$, and a total range of initial $^{87}Sr/^{86}Sr$ of 0.709–0.715. Isotopic studies of the Dovyren intrusion have also involved oxygen isotopes (Yaroshevsky et al., 1980; Krivopliasov et al., 1982, Krivopliasov et al., 1984) and have shown anomalously high and variable $\delta^{18}O$-values, between +6.5 and +14‰, with even higher $\delta^{18}O$ values (+15 to +20‰) in the magnesian skarns.

3. Samples and analytical procedures

Fifteen ~ 1-kg samples from the Dovyren intrusion were collected to represent the compositional range of the body. Sample localities are shown in Fig. 4, and their chemical compositions are presented in Table 1 and Fig. 5. Two mafic footwall sills and six metasedimentary country rocks were also sampled for the comparative study. Samples I-1 and I-2 were collected ~ 1 m from each other at the lower contact of the Dovyren intrusion and represent hornfelsed dolomitic marble from the exocontact and chilled marginal gabbronorite, respectively. Samples TST-23, TST-28 and TST-29 are schists reworked by contact metamorphism during emplacement of the Dovyren intrusion.

The samples, denoted D and TST, were collected by one of the authors (E.Yu.R), and the others were provided by E.V. Koptev-Dvornikov (Moscow State University). All samples of mafic and ultramafic rocks are fresh, with completely preserved igneous mineralogy. Weathering crusts were carefully removed before crushing. Mineral separates from samples D-2, D-9, D-28 and D-109 were prepared at the Institute of Precambrian Geology and Geochronology (IPGG) with conventional magnetic and heavy-

Table 1
Major- and rare-earth element data

Sample	IV-3	IV-12	IV-34	D-9	IV-48	IV-56	IV-64	D-8	D-6	IV-78	II-25	II-2	I-2	I-1	D-2	TST-24	TST-28
SiO_2 (wt%)	48.96	50.31	44.09	42.86	47.66	41.96	41.65	37.90	37.69	41.37	39.73	46.04	48.48	7.54	50.51	49.67	
TiO_2	0.56	0.37	0.10	0.07	0.12	0.02	0.02	0.04	0.07	0.02	0.03	0.32	0.45	0.02	0.58	0.75	
Al_2O_3	14.92	15.60	15.70	16.32	17.31	14.78	3.51	2.87	2.02	12.15	1.32	9.23	14.97	1.20	14.98	13.02	
FeO_{tot}	7.83	8.81	9.93	7.44	5.21	8.63	13.33	12.75	14.06	9.32	11.84	10.32	6.74	0.16	7.13	9.06	
MnO	0.14	0.16	0.14	0.12	0.09	0.12	0.19	0.21	0.20	0.12	0.17	0.15	0.11	0.02	0.14	0.16	
MgO	8.34	9.15	16.96	18.42	9.74	21.96	37.04	39.24	40.49	25.75	39.97	23.86	9.34	24.87	10.09	7.23	
CaO	10.91	11.29	9.94	10.38	16.56	7.82	1.71	2.32	1.32	6.94	1.99	5.96	9.51	30.80	11.91	14.75	
Na_2O	1.84	1.54	0.90	0.88	0.87	0.57	0.11	< 0.02	0.24	0.49	0.03	0.94	2.06	0.03	1.66	2.19	
K_2O	0.57	0.36	0.11	0.09	0.02	0.02	0.02	0.07	0.06	0.02	0.02	0.40	1.22	0.02	0.78	0.53	
P_2O_5	0.09	0.02	0.02	0.01	0.02	0.02	0.02	0.01	0.01	0.02	0.02	0.04	0.07	0.11	0.07	0.11	
mg #	0.651	0.645	0.750	0.813	0.766	0.817	0.830	0.844	0.835	0.829	0.856	0.802	0.708	0.996	0.712	0.583	
La (ppm)				1.393				0.725							12.85	12.94	
Ce				2.807				1.247	2.262						26.69	25.43	81.77
Nd				1.422				0.495	1.040						12.78	12.55	37.18
Sm				0.319				0.092	0.212						2.675	2.717	7.288
Eu				0.300				0.045	0.066						0.802	0.919	1.158
Gd				0.336				0.090	0.212						2.656	2.863	6.540
Dy				0.352				0.094	0.228						2.784	3.006	6.264
Er				0.216				0.072	0.154						1.706	1.863	3.474
Yb				0.212				0.095	0.176						1.591	1.770	3.293

liquid techniques. An additional hand-specimen of olivine gabbro D-9 was processed at the Royal Ontario Museum (ROM) where 2–4-mg pure fractions of plagioclase and clinopyroxene were separated by hand-picking.

Major-element concentrations were determined by conventional X-ray fluorescence (XRF) techniques at the IPGG. Rare-earth element (REE) concentrations were measured with isotope dilution techniques (Puchtel et al., 1993) at the Institute for the Geology of Ore Deposits, Petrography, Mineralogy and Geochemistry of the Russian Academy of Science, Moscow (IGEM). The accuracy and precision of REE determinations are ~ ±3% for La and Lu, and better than ±2% for the other REE.

All Nd-, Sr- and Pb-isotopic analyses were performed at the IPGG, except Nd and Pb analyses of an additional specimen of D-9 that were performed at the ROM. The following description refers to the analytical procedures used at the IPGG. Whole-rock powders and mineral separates weighing 50–200 mg were spiked with mixed ^{85}Rb–^{84}Sr and ^{149}Sm–^{146}Nd solutions and digested in screw-capped polytetrafluoroethylene (PTFE) capsules with HF–HNO_3 or HF–$HClO_4$ mixtures at 100°C for 1–3 days, then evaporated to dryness and redissolved in 2 *N* HCl. Rb, Sr and light REE (LREE) were separated using conventional cation-exchange techniques on quartz columns packed with 5 ml of Bio-Rad® AG 50W × 8 resin. Rb and Sr were eluted with 2 *N* HCl and

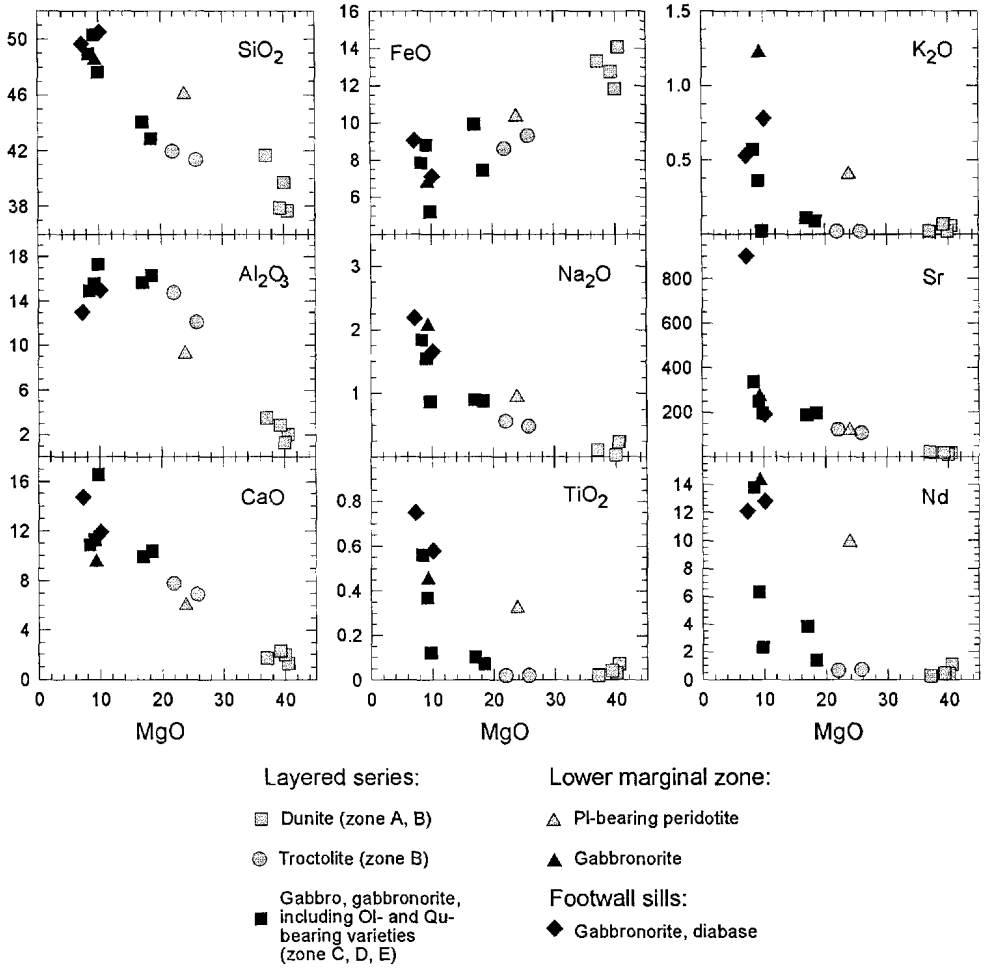

Fig. 5. Major-element compositions of the studied samples from different stratigraphic zones of the Dovyren intrusion and footwall sills.

Table 2
Sm–Nd and Rb–Sr analytical data and model parameters

Sample	Fraction	Sm (ppm)	Nd (ppm)	$^{147}Sm/^{144}Nd$	$^{143}Nd/^{144}Nd$ [a]	ε_{Nd} @ 673 Ma	Rb (ppm)	Sr (ppm)	$^{87}Rb/^{86}Sr$	$^{87}Sr/^{86}Sr$ [a]	$^{87}Sr/^{86}Sr$ @ 673 Ma
IV-1 hornfels	WR	5.08	25.9	0.1187	0.511704 ± 0.000006	−11.5					
IV-3 Qu gabbro	WR	2.91	13.8	0.1274	0.511559 ± 0.000004	−15.1	13.4	338	0.1146	0.71143 ± 0.00003	0.71033
IV-12 gabbronorite	WR	1.33	6.33	0.1274	0.511591 ± 0.000004	−14.5	8.38	249	0.0973	0.71131 ± 0.00002	0.71038
IV-34 Ol gabbro	WR	0.786	3.86	0.1229	0.511540 ± 0.000005	−15.1	3.52	190	0.0535	0.71287 ± 0.00002	0.71236
D-9 Ol gabbro	WR						1.33	198	0.0188	0.71250 ± 0.00006	0.71232
	Pl	0.151	1.14	0.0802	0.511350 ± 0.000020	−15.1	1.98	267	0.0206	0.71216 ± 0.00002	0.71196
	WR [c]	0.372	1.40	0.1607	0.511711 ± 0.000007	−15.0					
	Pl [c]	0.103	0.815	0.0764	0.511330 ± 0.000024	−15.2					
	Pl [c]	0.119	0.906	0.0797	0.511352 ± 0.000011	−15.0					
	Cpx [c]	1.186	3.67	0.1954	0.511861 ± 0.000007	−15.0					
IV-48 Ol gabbro	WR	0.596	2.29	0.1576	0.511744 ± 0.000006	−14.1	0.61	195	0.0091	0.71036 ± 0.00003	0.71027
IV-56 troctolite	WR	0.119	0.665	0.1083	0.511503 ± 0.000008	−14.5	0.69	124	0.0161	0.71170 ± 0.00002	0.71155
IV-64 dunite	WR	0.055	0.267	0.1235	0.511519 ± 0.000020	−15.5	0.44	20.8	0.0616	0.71209 ± 0.00003	0.71150
D-8 Pl-bearing dunite	WR	0.089	0.452	0.1199	0.511911 ± 0.000050	−7.6	1.05	19.5	0.1492	0.70740 ± 0.00002	0.70597
	WR rep	0.095	0.481	0.1186	0.511878 ± 0.000008	−8.1					
D-6 Pl-bearing dunite	WR	0.215	1.04	0.1243	0.511582 ± 0.000010	−14.4	1.68	17.4	0.2877	0.71305 ± 0.00002	0.71029
IV-78 troctolite	WR	0.162	0.759	0.1291	0.511601 ± 0.000007	−14.4	4.42	110	0.1161	0.71121 ± 0.00003	0.71010

II-25 dunite	WR	0.105	0.414	0.1531	0.511724 ± 0.000007	−14.1	0.49	11.2	0.1273	0.71432 ± 0.00003	0.71310
II-2 Pl peridotite	WR	2.02	9.87	0.1239	0.511546 ± 0.000007	−15.0	14.4	117	0.3571	0.71691 ± 0.00002	0.71348
I-2 gabbronorite	WR	2.83	14.3	0.1200	0.511464 ± 0.000006	−16.3	39.0	271	0.4176	0.71754 ± 0.00002	0.71353
I-1 dolomitic marble	WR	0.267	1.17	0.1382	0.512016 ± 0.000006	−7.1	0.070	91.0	0.0022	0.70808 ± 0.00002	0.70806
D-2 gabbronorite	WR	2.65	12.8	0.1247	0.511570 ± 0.000007	−14.6	24.2	192	0.3507	0.71576 ± 0.00002	0.71239
	Pl	0.943	6.42	0.0888	0.511388 ± 0.000005	−15.1	27.0	2943	0.256	0.71535 ± 0.00002	0.71289
	Opx	1.97	7.35	0.1612	0.511734 ± 0.000008	−14.6					
	Cpx-l	1.53	5.60	0.1652	0.511740 ± 0.000010	−14.8					
	Cpx-h	2.01	7.04	0.1725	0.511786 ± 0.000005	−14.5					
	Bt	0.831	4.55	0.1104	0.511501 ± 0.000015	−14.7	446	10.1	140.5	2.14410 ± 0.00005	
TST-24 diabase	WR	2.61	12.1	0.1303	0.511586 ± 0.000013	−14.8	36.0	903	0.1109	0.71457 ± 0.00002	0.71351
TST-23 schist	WR	8.35	44.9	0.1126	0.511677 ± 0.000014	−11.5					
TST-28 schist	WR	7.04	35.9	0.1184	0.511910 ± 0.000011	−7.4	165	157	2.932	0.74522 ± 0.00002	0.71707
TST-29 schist	WR	4.70	23.1	0.1233	0.511810 ± 0.000009	−9.8					
X-Yoko dolomitic marble	WR	0.629	3.03	0.1251	0.511839 ± 0.000011	−9.4	10.8	57.9	0.5209	0.71610 ± 0.00002	0.71110
BCR-1 [b]	WR	6.54	28.6	0.1383	0.512633 ± 0.000018		45.9	326	0.4080	0.70501 ± 0.00003	

WR = whole rock (rep = replicate); Pl = plagioclase; Cpx = clinopyroxene (l = light; h = heavy); Opx = orthopyroxene; Bt = biotite.

[a] The uncertainties are $2\sigma_m$.

[b] Average of 13 analyses for Sm–Nd and 4 analyses for Rb–Sr. The uncertainties are ±2 S.D.

[c] Analyses performed at the Royal Ontario Museum, Toronto. All the other analyses are from the Institute of Precambrian Geology and Geochronology, St. Petersburg.

LREE fractions were eluted with 4 *N* HCl. Nd and Sm were separated on 1-ml quartz or PTFE columns packed with hydrogen di-ethylhexyl phosphate (HDEHP) -coated Teflon® powder (modified from Richard et al., 1976). Samples were loaded in 0.1 *N* HCl; Nd and Sm were eluted with 0.2 *N* HCl and 0.4 *N* HCl, respectively. The procedure blanks were ~ 50 pg Rb, 600 pg Sr, 70 pg Sm and 300 pg Nd.

The isotopic analyses were performed in static mode on a Finnigan® MAT 261 mass spectrometer equipped with variable 8-collector system. The Nd peaks were measured at masses 143, 144, 145, 146, 148 and 150. Fractionation correction used $^{148}Nd/^{144}Nd = 0.24157$; reported $^{143}Nd/^{144}Nd$ ratios are relative to $^{143}Nd/^{144}Nd = 0.511860$ in La Jolla standard. Fractionation and spike corrected $^{145}Nd/^{144}Nd$ and $^{150}Nd/^{144}Nd$ ratios were calculated in each run to ensure data quality. Possible Sm interferences were monitored on mass 147 but 147/144 ratios during Nd runs were always lower than 10^{-5} and typically no detectable signals on mass 147 were found. Approximately 70–100 individual ratios were taken within each run, resulting in internal precision of ±0.003% or better when the ^{144}Nd intensity was higher than 10^{-11} A. The external precisions are ±0.004% for $^{143}Nd/^{144}Nd$ and ±0.5% for $^{147}Sm/^{144}Nd$ based on replicate analyses of standard rocks. The precisions reported hereafter correspond to 95% confidence level. The mean values of 13 analyses of BCR-1 are listed in Table 2.

Sr-isotopic ratios were normalized to $^{88}Sr/^{86}Sr = 8.37521$. The mean $^{87}Sr/^{86}Sr$ for NBS SRM-987 is 0.710244 ± 0.000015 on 4 runs. Both internal and external precisions for $^{87}Sr/^{86}Sr$ are ±0.005% and the external precision for $^{87}Rb/^{86}Sr$ is ±0.5%. The mean values for BCR-1 standard are listed in Table 2.

Pb was separated from whole rock and plagioclase by anion exchange in HBr following Manhes et al. (1978). Plagioclase fractions were washed with 1 *N* HNO_3 to remove surface contamination. Powdered plagioclase was additionally subjected to "strong" (12 *N* HNO_3 for 5–6 hr on a hot plate) acid leaching, to remove possible radiogenic Pb components. Total blank of the common Pb procedures was 5 ± 2 ng Pb. Isotopic analysis of lead was carried out with the aid of silicate emitter. The mass-discrimination of 0.0013 ± 0.0003 amu^{-1}, determined by numerous measurements of NBS standard SRM-982, was used to correct for fractionation in the samples. Average values for NBS-982 measured during the course of these analyses are $^{206}Pb/^{204}Pb = 36.643$, $^{207}Pb/^{204}Pb = 17.092$ and $^{208}Pb/^{204}Pb = 36.551$. Estimated errors based on between-run precision of the standard are ±0.04% per amu, within-run precision for individual Pb analyses was typically ±0.004–0.01%.

Nd and Pb analytical procedures at the ROM are similar to those described by Heaman and Machado (1992), with a few changes summarized below. Total procedure blanks for Nd, Sm, Pb and U were 30, 15, 5 and 0.25 pg, respectively. Nd was loaded on single Re filaments with SiO_2 gel following Thirlwall (1991) and analyzed as NdO^+ ions in dynamic multicollector mode. Oxygen isotopic ratios $^{18}O/^{16}O = 0.00214$ and $^{17}O/^{16}O = 0.000397$, measured using $^{150}NdO^-$ ion beam, were used for oxygen isotope correction. Nd-isotopic ratios are normalized to $^{146}Nd/^{144}Nd = 0.7219$, and $^{143}Nd/^{144}Nd$ ratios are reported relative to $^{143}Nd/^{144}Nd = 0.511860$ in La Jolla standard. Uncertainties of individual analyses were propagated to include within-run precisions, external reproducibility of ±0.003% for $^{143}Nd/^{144}Nd$ and ±0.3% for $^{147}Sm/^{144}Nd$ based on replicate analyses of BCR-1, and uncertainties of Nd and Sm blanks.

Data regressions have been performed using the Isoplot© program (Ludwig, 1992). Nd-isotopic compositions are given in the ε_{Nd} notation as proposed by DePaolo and Wasserburg (1976) with values calculated using the CHUR (chondritic uniform reservoir) parameters of Jacobsen and Wasserburg (1980).

4. Results

4.1. Major-and trace-element concentrations

Major-element chemistry of the Dovyren intrusive rocks and footwall sills (Table 1; Fig. 5) covers almost the entire range of compositions typical for layered intrusions (Wager and Brown, 1967; Parsons, 1986). Dunite in zones *A* and *B* contains 37–40.5 wt% MgO and is very low in CaO, Al_2O_3, TiO_2, Na_2O and K_2O. The abundances of CaO, Al_2O_3 and Na_2O, elements which are compatible in

plagioclase, increase gradually with the decreasing MgO from dunite to troctolite and olivine gabbro. The abundances of TiO_2 and K_2O in troctolite are similar to those in dunite or even lower, and increase only slightly in olivine gabbro. Gabbroic rocks of zone *E* have the highest SiO_2, CaO, TiO_2, Na_2O and K_2O, and the lowest MgO and FeO in the layered series, while the abundance of Al_2O_3 reaches maximum values in olivine gabbro (zones *C* and *D*) and slightly decreases in zone *E*. Compositions of mafic rocks in the lower marginal zone and in footwall sills are comparable to those in zone *E*. Plagioclase-bearing peridotite from the lower marginal zone (sample II-2) has similar MgO and CaO abundances to troctolites in zone *B*, but considerably higher SiO_2, TiO_2 and K_2O and lower Al_2O_3.

The concentrations of Sr and Nd against MgO content are also shown in Fig. 5. Variations of Sr concentrations are similar to those of major elements, compatible in plagioclase, namely CaO and Na_2O. Variations of Nd resemble those of K_2O and TiO_2. An anomalously high Sr concentration in the diabase TST-24, 903 ppm, is much higher than in other samples from the Dovyren intrusion or footwall sills.

REE distributions were analyzed in three rocks from the layered series, two samples from footwall mafic sills, and one country rock schist (Table 1. The REE pattern for the country rock sample TST-28 is similar to that for the average post-Archean Australian shale (PAAS), taken by Taylor and McLennan (1985) to represent average upper continental crust. REE concentrations in mafic and ultramafic samples vary over a factor of 30 and have variable Eu anomalies that range from weakly negative to strongly positive. However, all these samples show similar strong enrichment in LREE relative to middle REE (MREE) and heavy REE (HREE) (Fig. 6). The concentrations of REE in mafic rocks from footwall sills (TST-24 and D-2) are ~ 3 times lower than in the schist TST-28, but the REE distributions are similar to the pattern for the schist, except that no pronounced Eu anomaly is observed in the mafic sill samples. Olivine gabbro D-9 has REE concentrations ~ 8 times lower than in samples TST-24 and D-2 and shows strong positive Eu anomaly. Plagioclase-bearing dunites D-6 and D-8 are distinguished by relative HREE enrichment, which, in combination with the LREE enrichment mentioned above, results in a U-shaped REE pattern.

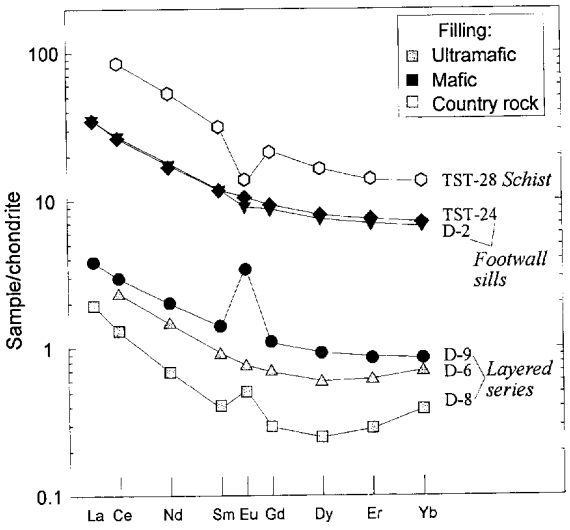

Fig. 6. Chondrite-normalized REE patterns for three ultramafic–mafic cumulates, two rocks from mafic sills and an enclosing schist. Chondritic REE concentrations are after Taylor and McLennan (1985).

4.2. Age of the intrusion

We attempted to determine the crystallization age of Dovyren intrusion by Sm–Nd and Rb–Sr internal isochron methods. In contrast to the whole-rock isochron approach, internal isochron dating does not require uniformity of initial isotopic ratios between samples, and the calculated ages are insensitive to possible variable contamination. Sm–Nd and Rb–Sr data for whole rocks and mineral separates are presented in Table 2. Sm–Nd internal isochrons for an olivine gabbro (D-9) from zone *D* and a gabbronorite (D-2) from a sill injected into schists and sandstones beneath the Dovyren intrusion are shown in Fig. 7; the ages of 673 ± 22 and 707 ± 40 Ma, respectively, are within error of each other. However, the ages of the main intrusion and associated sills may be slightly different, as was demonstrated by U–Pb dating of the Stillwater intrusion and associated footwall mafic sills (Premo et al., 1990). Because of the possible age difference between the intrusion and sills, we prefer the internal isochron age for olivine gabbro D-9 673 ± 22 Ma as the best

estimate of the crystallization age of the Dovyren intrusion. Rb–Sr age of biotite from the gabbronorite D-2, calculated relative to the whole rock or plagioclase, is 713 ± 7 Ma (uncertainty is based on analytical precision of $^{87}Rb/^{86}Sr$ and $^{87}Sr/^{86}Sr$ ratios), and is 5.7% higher than the preferred Sm–Nd mineral isochron age.

4.3. Sr- and Nd-isotopic variations

The Dovyren intrusion is characterized by low and uniform initial Nd-isotopic ratios, and high and variable initial Sr-isotopic ratios, calculated for the age of 673 Ma. The initial Sr- and Nd-isotopic values are plotted in Fig. 8 against the stratigraphic position in the cross-section of the Dovyren intrusion. With two exceptions, the $\varepsilon_{Nd}(T)$-values in samples from the Dovyren intrusion and sills are nearly constant, within the limits of -14.8 ± 0.7. The marginal gabbronorite I-2 has slightly lower $\varepsilon_{Nd}(T) = -16.3$, and the plagioclase-bearing dunite D-8 has $\varepsilon_{Nd}(T) = -8.1$, significantly higher than most samples. Strontium initial isotopic ratios vary from 0.7101 to 0.7135 and form a series of distinct groups with relatively uniform initial ratios within each group. The higher Sr initial ratios 0.71310–0.71353 are observed in the lower marginal zone and the dunite zone, and in diabase TST-24 collected

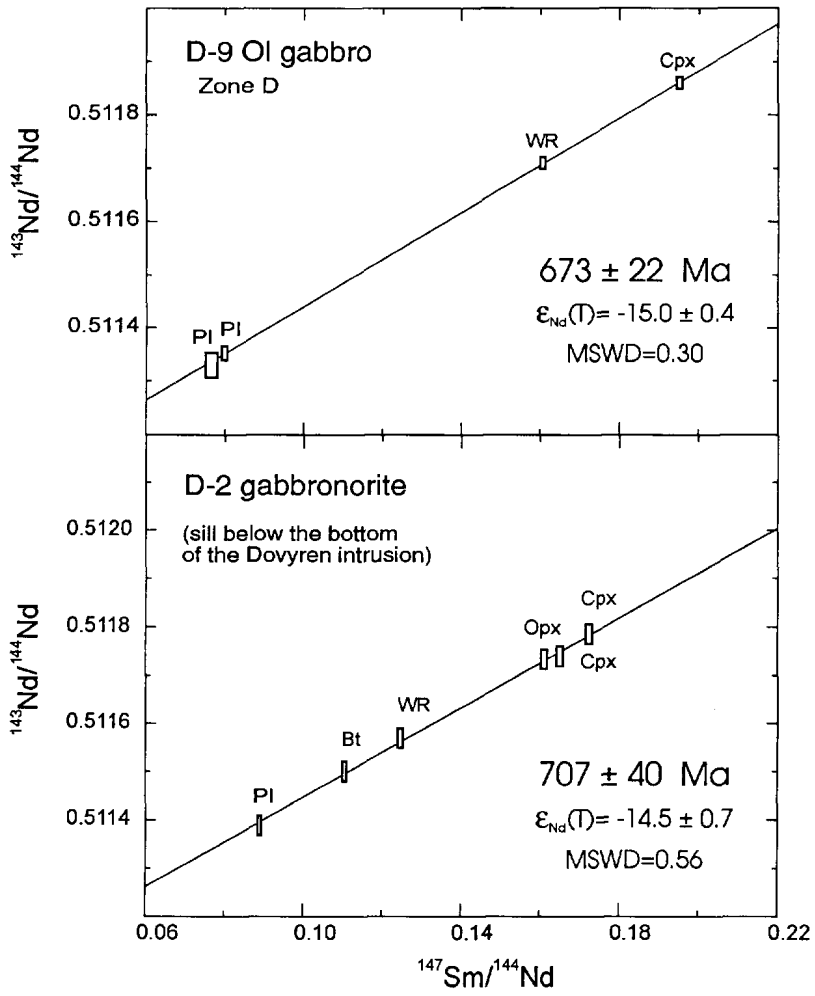

Fig. 7. Internal Sm–Nd isochrons for the olivine gabbro D-9 and gabbronorite D-2.

from a sill near the base of the intrusion. Samples from zones *C* and *E*, and two samples from the lower part of zone *B*, have Sr initial ratios within the range of 0.71010 to 0.71038. Two samples from the upper part of zone *B* have Sr initial ratios of 0.71150 to 0.71155, and two samples from zone *D* have Sr initial ratios 0.71232 and 0.71236. The sample D-8 (plagioclase-bearing dunite from zone *B*) has $\varepsilon_{Nd}(T) = -8.1$ (more precise of two replicate analyses, Table 2) and Sr initial ratio of 0.70597, very different from those for all the other rocks of the Dovyren massif studied here.

Country rocks exhibit a wide range of variations of initial $^{87}Sr/^{86}Sr$. Lower values of 0.70806 and 0.71110 are observed in dolomitic marbles I-1 and X-Yoko, respectively, and the schist TST-28 has Sr initial ratio of 0.71707. ε_{Nd}(673 Ma) in two dolomitic marbles, three schists and a hornfels IV-1 range from −11.5 to −7.1, without systematic difference between silicate and carbonate metasedimentary rocks.

4.4. Pb-isotopic results

Lead isotopic data for three samples of baked schists, collected within the contact aureole of the Dovyren intrusion, and their acid leachates and residues (Table 3; Fig. 9a and b), indicate systematic differences between acid-soluble and insoluble components of these rocks. The Pb-isotopic compositions of residues are more radiogenic than that of the whole rocks, while the leachates contain less radiogenic Pb, opposite to what is commonly observed (Neymark, 1987). This unusual distribution of radiogenic Pb components is possibly a result of preferential dissolution of low-U/Pb minerals, most likely sulfides, during acid treatment. Acid leachates, residues and untreated samples together define a linear array with MSWD = 1.4 in the $^{207}Pb/^{204}Pb$–$^{206}Pb/^{204}Pb$ coordinates (Fig. 9a). The absence of correlation in the $^{208}Pb/^{204}Pb$–$^{206}Pb/^{204}Pb$ coordinates (Fig. 9b) precludes the interpretation of the

Table 3
Pb-isotopic data

Sample	Fraction	Leaching	U (ppm)	Pb (ppm)	$^{238}U/^{204}Pb$	$^{206}Pb/^{204}Pb$	$^{207}Pb/^{204}Pb$	$^{208}Pb/^{204}Pb$
Mafic rocks of the Dovyren intrusion and footwall sills:								
D-28	Pl	residue				16.803	15.481	37.166
D-109	Pl	leachate				17.322	15.526	37.837
		residue				16.916	15.480	37.558
D-9	Pl	leachate				17.218	15.550	37.702
		residue				17.090	15.480	37.364
		residue [a, c]	0.0074	0.369	1.222	16.903	15.477	37.473
		residue [b, c]	0.0051	0.354	0.881	16.896	15.481	37.445
D-2	Pl	leachate				17.184	15.524	37.693
		residue				17.136	15.501	37.586
Country rocks:								
TST-23	WR					20.672	15.752	40.977
		leachate				19.430	15.698	40.908
		residue				25.726	16.074	41.436
TST-28	WR					20.309	15.734	40.539
		leachate				18.956	15.653	40.328
		residue				25.267	16.065	41.484
TST-29	WR					21.706	15.811	41.931
		leachate				19.976	15.719	40.814
		residue				23.844	15.958	42.562

[a] Hand-picked fraction of best clear grains.
[b] Bulk plagioclase fraction, variable quality of grains.
[c] Fractions analyzed at the ROM, all the other analyses are from the IPGG.

$^{207}Pb/^{204}Pb$–$^{206}Pb/^{204}Pb$ array as a mixing line, so it is likely to represent a geologically meaningful isochron. The age of 713 ± 120 Ma is within error of the Sm–Nd mineral isochron age for the Dovyren intrusion.

Pb-isotopic data for acid-leached plagioclases from the Dovyren mafic rocks (Table 3; Fig. 9c and d), occupy a restricted field of $^{206}Pb/^{204}Pb$ between 16.80 and 17.14, and $^{208}Pb/^{204}Pb$ between 37.17 and 37.59. $^{207}Pb/^{204}Pb$ ratios, from 15.477 to 15.501, are within analytical uncertainty. The Pb-isotopic composition of leachates is slightly more radiogenic than that of residues. $^{238}U/^{204}Pb$ (μ) of 0.88 and 1.22 in two leached plagioclase fractions from the olivine gabbro D-9 indicative of the presence of a small amount of radiogenic Pb, may produce an excess of 0.09–0.13 in $^{206}Pb/^{204}Pb$, and negligible excess of 0.006–0.008 in $^{207}Pb/^{204}Pb$. The correction for in situ U decay was not applied, however, because $^{238}U/^{204}Pb$ in plagioclase may be biased by acid leaching (Amelin and Neymark, 1995). The least radiogenic $^{206}Pb/^{204}Pb$ in the plagioclases is similar to the 673-Ma value in the model depleted mantle, DM (Zartman and Haines, 1988), but $^{207}Pb/^{204}Pb$ and $^{208}Pb/^{204}Pb$ are substantially higher than the DM values. On a $^{207}Pb/^{204}Pb$–$^{206}Pb/^{204}Pb$ plot (Fig. 9c) analytical points of the plagioclases plot near the S–K (Stacey and Kramers, 1975) model growth curve, but are shifted towards model age values, more ancient than the age of the intrusion.

5. Discussion

5.1. Composition of the parental magma

The correct evaluation of a parental magma composition is important to constrain contamination models, as well as petrogenetic models in general (here we use the term "parental magma" for the magma, emplaced into the magma chamber, and

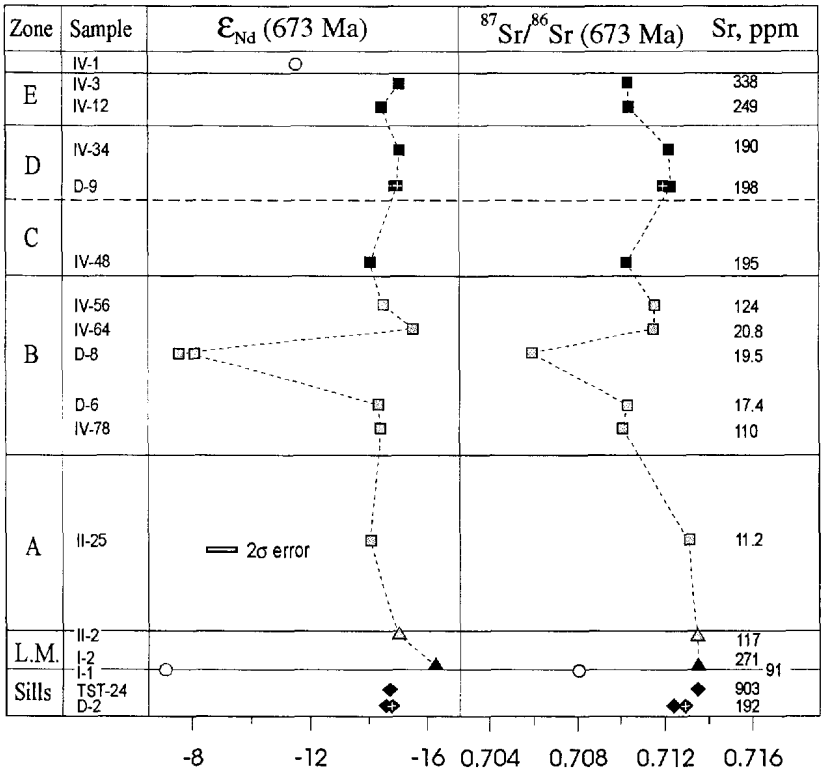

Fig. 8. Variations of initial ε_{Nd} and $^{87}Sr/^{86}Sr$ values (at 673 Ma) and Sr concentrations through the cross-section of the Dovyren intrusion.

possibly already contaminated; the term "primary magma" is reserved for a hypothetical magma composition before contamination). If a magma chamber behaves as a closed system after injection of parental magma (or magmas), i.e. no tapping of residual melt occurs, then the average composition of an intrusion corresponds to the average compositions of parental magmas. However, if a residual melt was removed from the magma chamber, then the abundance of components, concentrating in early cumulus minerals, may be grossly overestimated, in particular MgO and FeO because of accumulation of olivine. In addition, if parental magma, initially injected into the chamber, contained phenocrysts, then the average composition of an intrusion that crystallized under closed-system conditions would reflect the composition of magmatic liquid plus phenocryst mixture, rather than the composition of the magmatic liquid alone. The composition of parental magma can be directly estimated from the composition of chilled marginal rocks, but this estimate may be subject to a large degree of uncertainty if the magma contained abundant phenocrysts.

The average composition of the Dovyren intrusion, calculated by Yaroshevsky et al. (1983), is that of an ultramafic magma (26.6 wt% MgO and 44.5 wt% SiO_2, Table 4 , within the compositional range of peridotitic komatiites. The average composition of "chilled margins", reported by Yaroshevsky et al. (1983), is only slightly lower in magnesium (24.7 wt% MgO). However, the presence of olivine phenocrysts suggests that this composition is probably higher in MgO than the parental magmatic liquid. The estimated MgO content of a parental magma of a peridotite sill near the bottom of the Dovyren intrusion is 15.7 wt% MgO, assuming 30% olivine

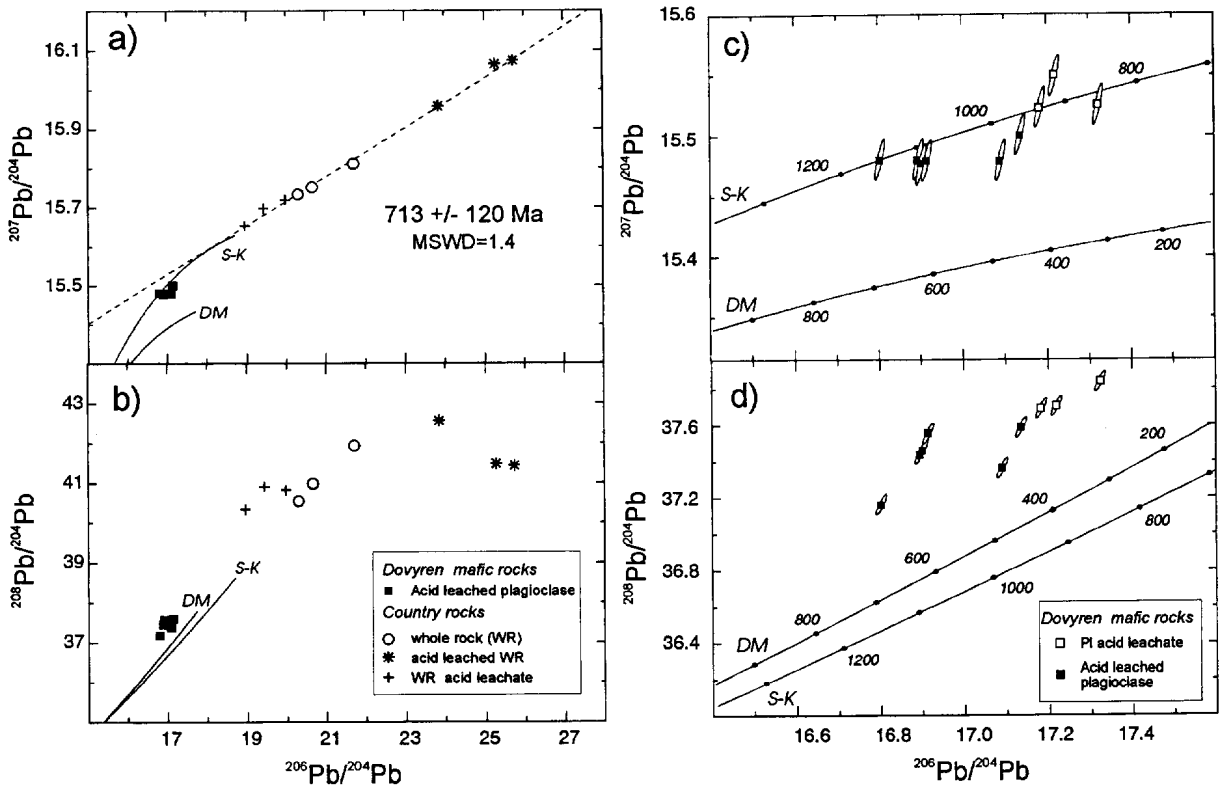

Fig. 9. $^{207}Pb/^{204}Pb$ vs. $^{206}Pb/^{204}Pb$ (a) and $^{208}Pb/^{204}Pb$ vs. $^{206}Pb/^{204}Pb$ (b) plots for plagioclases from the Dovyren mafic rocks, and whole-rock samples of baked contact sediments, their acid leachates and residues after leaching. Evolution curves are from Stacey and Kramers (1975) for the average continental crust and from Neymark (1990) for the depleted mantle.
c and d. Pb isotope data for acid leachates and residues of plagioclases from the Dovyren mafic rocks.

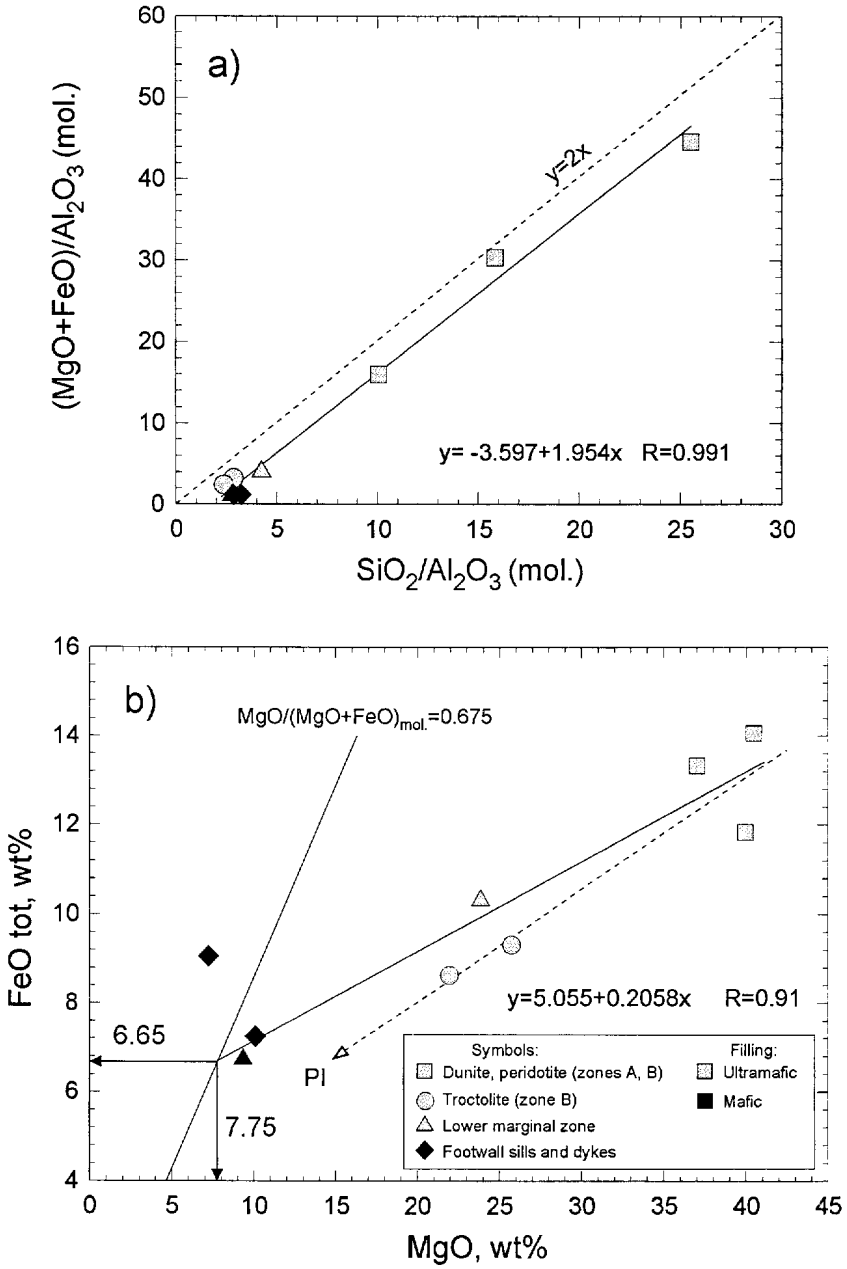

Fig. 10. a. Pearce (1968) plot of molecular ratio $(MgO + FeO)/Al_2O_3$ vs. SiO_2/Al_2O_3. The slope close to the $(MgO + FeO)/SiO_2 = 2$ in olivine indicates olivine-controlled fractionation in the lower marginal zone and in dunites in zones *A* and *B*. Data for troctolites from zone *B* and gabbroids from the sills are shown for comparison, but are not included in the regression.

b. MgO–FeO variation diagram showing the regression for dunites from zones *A* and *B*, and samples from the lower marginal zone. Intersection with the line of constant mg # = 0.675 yields MgO = 7.75 wt% and FeO = 6.65 wt% in the magma. The troctolite and sill points are not included in the regression. The troctolite points plot along the olivine–plagioclase mixing line (*dashed arrow*), pointing to the plagioclase composition MgO = 0, FeO = 0.

accumulation (Papunen et al., 1992). This value is interpreted by Papunen et al. (1992) as a minimum MgO content for the parental magma of peridotite sills and the Dovyren intrusion. A potential problem with this approach is the uncertainty in the content of olivine phenocrysts.

An alternative approach is to use the olivine composition to infer the MgO/FeO in the magma in equilibrium with olivine. The calculated MgO/FeO in the magma, however, may be too low, if cumulus olivine re-equilibrated with intercumulus liquid (Barnes, 1986; Chalokwu and Grant, 1987). The most magnesian olivine compositions in the Dovyren intrusion (Fo 87.2–87.5) from two dunite samples in zone *A* (Ionov et al., 1984a), are similar in composition to an olivine inclusion in chromite from a dunite in the lower marginal zone (Kislov, 1990), which was protected from re-equilibration by the enclosing chromite. Using these analyses and the Fe–Mg exchange coefficient between olivine and melt at low pressure $K_D = (FeO/MgO)_{Ol}/(FeO/MgO)_{melt} = 0.3 \pm 0.03$ (Roeder and Emslie, 1970), the mg # [molar MgO/(MgO + FeO)] of melt in equilibrium with the olivine is 0.675. A much higher mg # = 0.807, calculated for the "average chilled margin" (Table 4 , agrees more closely with the presence of large amount of phenocrystic olivine.

On the basis of the inferred mg # in the parental magma, we can estimate MgO and FeO contents from the positive FeO–MgO correlation for the rocks, composed mainly of solidified parental melt and phenocrystic and/or cumulus olivine with a minimum amount of other cumulus minerals (Chai and Naldrett, 1992). Regression through five analytical points (a plagioclase-bearing peridotite and gabbronorite from the lower marginal zone, and three dunites), intersects the line of constant mg # = 0.675 at 7.75 wt% MgO and 6.65 wt% FeO (Fig. 10b). These values may be underestimated, due to the possible presence of plagioclase phenocrysts in addition to olivine phenocrysts. The effect of plagioclase presence is illustrated by the troctolite analyses,

Table 4
Calculated average compositions of the Dovyren intrusion, compared to the compositions of rocks in the lower marginal zone and footwall sills

Sample	II-2	I-2	D-2	TST-24	Average of col. 2–4	Dovyren average [a]	Average margin [b]	Estimated parentalmagma [c]	Alternative parentalmagma [d]
Column	1	2	3	4	5	6	7	8	9
SiO_2 (wt%)	46.04	48.48	50.51	49.67	49.5	544.54	47.71	49.82	47.30
TiO_2	0.32	0.45	0.58	0.75	0.59	0.09	0.36	0.49	0.38
Al_2O_3	9.23	14.97	14.98	13.02	14.32	10.64	9.11	15.84	12.42
ΣFeO	10.32	6.74	7.13	9.06	7.64	10.05	10.37	6.65	8.29
MnO	0.15	0.11	0.14	0.16	0.14	0.14	0.15		
MgO	23.86	9.34	10.09	7.23	8.89	26.57	24.75	7.75	15.70
CaO	5.96	9.51	11.91	14.75	12.06	7.35	6.03	10.00	7.89
Na_2O	0.94	2.06	1.66	2.19	1.97	0.54	0.94	2.08	1.58
K_2O	0.40	1.22	0.78	0.53	0.84	0.07	0.54	1.18	0.88
mg #	0.802	0.708	0.712	0.583	0.662	0.823	0.807	0.675	0.772
Nd (ppm)	9.87	14.3	12.8	12.1	13.07			15.83	12.07
Sm	2.02	2.83	2.65	2.61	2.70			3.147	2.40
Rb	14.4	39.0	24.2	36.0	33.1			38.3	28.7
Sr	117	271	192	903	455			271	206

[a] Average composition of the Dovyren intrusion from Yaroshevsky et al. (1983).
[b] Average composition of "chilled" margin from Yaroshevsky et al. (1983).
[c] Composition of the Dovyren parental melt, estimated from correlations between MgO and other major and trace components in 3 dunites and 2 rocks from the lower marginal zone (see text for details). MgO concentration is determined from FeO–MgO correlation and the most magnesian olivine composition (Fig. 10b), assuming that magma and olivine are in equilibrium.
[d] Alternative composition of the Dovyren parental melt, estimated from correlation between MgO and other major and trace components in 3 dunites and 2 rocks from the lower marginal zone, using the MgO concentration estimated by Papunen et al. (1992).

shown in Fig. 10b but not included in the regression. However, the correlation of molecular ratios (MgO + FeO)/Al_2O_3 vs. SiO_2/Al_2O_3 (Fig. 10a) with slope of 1.95, close to the theoretical value of 2 for olivine fractionation, indicates that the role of plagioclase fractionation was probably small.

The contents of SiO_2, CaO and other major and trace elements in the lower marginal rocks and dunites are strongly negatively correlated with MgO (correlation coefficients between −0.99 and −0.91), and the contents of these elements in the parental melt were estimated from regressions using the same set of analyses, at 7.75 wt% MgO. Overall, the calculated parental Dovyren magma composition (Table 4) is a basalt, similar to a normal type mid-ocean ridge basalt (N-MORB; e.g., Sun et al., 1979)

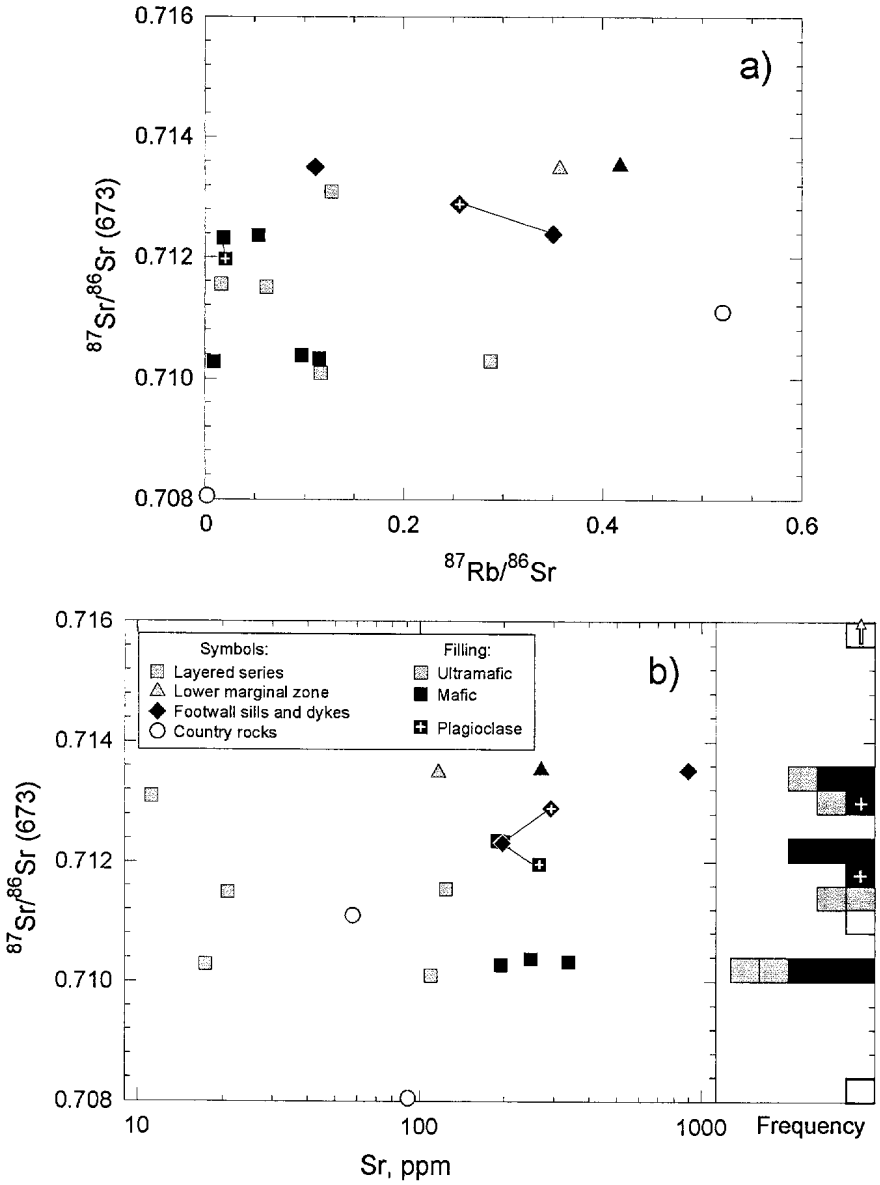

Fig. 11. Initial $^{87}Sr/^{86}Sr$ in whole-rock samples and plagioclase fractions, plotted against $^{87}Rb/^{86}Sr$ (a) and Sr concentrations (b). The histogram shows the distribution of initial $^{87}Sr/^{86}Sr$ ratios.

in SiO_2, MgO, Al_2O_3 and Na_2O contents, but poorer in TiO_2 and richer in K_2O, Rb, Sr and REE. This parental magma composition is close to the compositions of mafic rocks of the lower marginal rocks and the sills, in particular, gabbronorites I-2 and D-2. The uncertainty of the inferred parental magma composition is rather large (20–45% range of variations for different major and trace elements at 1σ confidence level), due to the small number of analyses included in regressions. If strong correlations in MgO variation diagrams hold with a larger number of analyses, a more precise estimate of the magma composition could probably been obtained.

5.2. *Significance of isotopic variations within the Dovyren intrusion*

With one notable exception, initial Nd-isotopic ratios of samples from the Dovyren intrusion are nearly constant ($\varepsilon_{Nd}(T)$ from -16.3 to -14.1), whereas the initial Sr ratios vary from 0.7101 to 0.7135. Apparently, processes that caused variations in the Sr-isotopic composition did not affect the Nd-isotopic signature. The incoherent behavior of Sr- and Nd-isotopic systems may be partly due to alteration effects, because the Rb–Sr isotopic system in basic rocks is more sensitive to a low-temperature hydrothermal alteration than the Sm–Nd system (Richardson, 1984; Hergt et al., 1989). The processes that might have caused the post-crystallization variations in the Sr-isotopic ratios are open-system behaviour shortly after crystallization (e.g., fluid exchange with enclosing rocks during cooling of the intrusion) and disturbance of the Rb–Sr system during ~ 550-Ma regional metamorphism (Neymark et al., 1991b). The consistency of the Sm–Nd mineral isochron age (707 ± 40 Ma) and Rb–Sr biotite age (713 ± 7 Ma) for the gabbronorite D-2 provides evidence against the metamorphic disturbance of the Rb–Sr system. Other post-crystallization effects, such as fluid exchange between the intrusion and country rocks, cannot be ruled out by these data.

If the Rb–Sr system was not disturbed during regional metamorphism, then the variations in Sr initial ratios between magmatic minerals or between a mineral and a whole rock may provide a good test for the post-crystallization open-system behavior on the mineral scale. The differences in initial $^{87}Sr/^{86}Sr$ between plagioclase fractions and whole-rock samples, 0.00036 for the olivine gabbro D-9 and 0.00050 for the gabbronorite D-2 (Table 2; Fig. 11a and b), indicate that at least some part of the Sr-isotopic variations is the result of post-crystallization open-system behavior, and reflect the minimum magnitude of alteration effect on Sr-isotopic ratios (which is ~ 10–15% of the range of the whole-rock initial $^{87}Sr/^{86}Sr$ variations).

The possibility that the entire range of initial Sr variations in the Dovyren intrusion is a result of alteration cannot be excluded, but is unlikely because of the following reasons. First, dunites, troctolites and gabbroic rocks show similar ranges of initial Sr variations, despite a more than 30-fold variation in Sr concentrations (from 11.2 ppm in dunite II-25 to 338 ppm in quartz-bearing gabbro IV-3, Fig. 11b). If the Sr-isotopic variations are the result of alteration, then a hypothetical alteration mechanism should provide either fluid/rock ratios, or concentrations of Sr in the fluid proportional to the Sr concentration in the rock with which the fluid interacts. Not to mention that it should be a rather unusual alteration mechanism, there is no evidence for stronger post-solidification alteration in the gabbroic rocks than in the peridotites. Second, the Sr initial ratios cluster in a few groups (Figs. 8 and 11b). A group of 3 samples with higher initial Sr ratios between 0.71310 and 0.71353 is restricted to the lower marginal zone and the dunite zone, while the samples from zones *C* and *E*, and two samples from the lower part of the zone *B*, have lower initial Sr ratios of 0.71010–0.71038. Variations of initial ratios within the groups do not exceed the probable alteration-related variations, estimated from the plagioclase–whole rock data, while the difference between the groups is ~ 7–11 times larger than the variations within the groups. We thus conclude that the observed variations in the initial Sr ratios are not completely a result of alteration, but are real and were generated at the magmatic stage.

The plagioclase-bearing dunite D-8 has $\varepsilon_{Nd}(T) = -8.1$ and $I_{Sr} = 0.70597$, very different from those for all other studied rocks of the Dovyren intrusion. The isotopic data are in agreement with two possible hypotheses about the origin of the plagioclase-bearing dunite D-8: assimilation either of ultramafic, or of

magnesian carbonate rocks, present among the country rocks before the emplacement of the Dovyren intrusion.

The plagioclase-bearing dunite may represent one of a group of metaperidotite bodies widespread in the Olokit trough, partially assimilated by the Dovyren magma. Two samples of metaperidotite from the Avkit massif (Fig. 2) were analyzed for Sr and Nd isotopes giving ε_{Nd}(673 Ma) +0.7 and +2.9 and I_{Sr}(673 Ma) 0.7061 and 0.7055 (Yu.V. Amelin, unpublished data, 1994). This possibility is difficult to check, because the peridotites of the Baikal area are heterogeneous and strongly serpentinized, so the values measured in the Avkit massif here may not be representative and/or affected by alteration.

Another mechanism that could possibly produce the plagioclase-bearing dunite is thermal decomposition and assimilation of a dolomite layer by basaltic magma. The geological evidence for this possibility is indicated by the presence of apodolomitic magnesian skarns in the dunitic zone. The initial Sr and Nd values in D-8 are much closer to those in the two samples of carbonate country rocks (dolomitic marbles X-Yoko and I-1), than to the other rocks of the Dovyren intrusion (Table 2).

Although Sr- and Nd-isotopic data cannot distinguish between these possibilities, major-element data provide some constraints. Peridotites formed by assimilation may differ in major-element and modal compositions from peridotites formed by crystal accumulation. Assimilation of a dolomite with CaO/MgO = 1.2–1.4 and very low FeO (analyses of the Dovyren country rock dolomites from Gurulev (1983), and dolomitic marble I-1 in Table 4) would probably result in formation of lherzolite or wehrlite with high CaO content and very high mg # and containing abundant magnesian diopside. These features are characteristic of apodolomitic magnesian skarns in the Dovyren intrusion, studied by Gurulev (1983). However, none of these features are observed in the sample D-8, which has major-element contents and modal composition within the range of other plagioclase-bearing dunites of the zone *B*. On the other hand, the possibility of dunite formation through the interaction between peridotite and basaltic magma was demonstrated by Kelemen et al. (1992, 1995). We thus prefer the model of peridotite assimilation for the origin of the isotopically distinct plagioclase-bearing dunite.

5.3. Contamination in the magma chamber

The distinctive initial isotopic features of the Dovyren rocks: low initial ε_{Nd}, high $^{87}Sr/^{86}Sr$ and $^{207}Pb/^{204}Pb$, provide strong evidence for the involvement of ancient LILE- (large ion lithophile element) and LREE-enriched material during magma genesis. The initial ε_{Nd}-values are significantly lower than the values of magmas derived from oceanic mantle (Zindler and Hart, 1986), and are comparable to the lowest ε_{Nd}-values observed in continental flood basalts (Hawkesworth et al., 1984; Cox and Hawkesworth, 1985). Moreover, initial ε_{Nd} of the Dovyren rocks are lower than in any analyzed metasedimentary country rocks. This, of course, does not exclude the possibility of contamination in the magma chamber. However, if such contamination did occur, it must have changed ε_{Nd} to less negative values, and the magma before emplacement had even lower ε_{Nd} than the values of ~ -14.8, observed in the Dovyren intrusion. The possible magnitude of contamination in the magma chamber can be estimated from the Nd-isotope data. If we take $\varepsilon_{Nd} = -16.1$ in the "chilled" marginal gabbronorite I-2 as representative for the magma at the time of emplacement, $\varepsilon_{Nd} = -9.6$ and [Nd] = 34.6 ppm (average of 3 silicate country rocks) as a contaminant signature, and $\varepsilon_{Nd} = -14.8$, [Nd] = 15.8 ppm for the contaminated magma (Table 4, column 8), then a simple mixing calculation yields a 9% mass fraction of the contaminant and the Nd concentration of 13.9 ppm in the emplaced magma. Concentration and isotopic effects of contamination in the magma chamber thus estimated are small (~ 12% and 1.3 ε-units, respectively), and do not significantly alter the further considerations of the contamination and/or enrichment processes before magma emplacement.

We think, however, that even this estimate of the degree of in situ contamination is too high. The uniformity of initial Nd-isotopic compositions in the Dovyren intrusion (except I-2 and D-8) implies that, if contamination in the magma chamber occurred, then the magma would have been perfectly homogenized by convection after contamination. The variations of initial Sr-isotopic ratios throughout the intru-

sion indicate that this was not the case. In addition, the similar ε_{Nd}-values in the Dovyren intrusion and the footwall sills require similar amounts of contamination for the magma chamber and the sills. We therefore conclude that contamination in the magma chamber was probably a local process, and its effect on the overall isotopic and chemical composition of the magma was minimal, so initial isotopic ratios in

Table 5
Models of magma contamination (simple mixing)

Column	Primitive picritic basalt 1	PAAS 2	Average upper crust 3	Proportion of mixing 1 4	Proportion of mixing 2 5	Contaminated magma 1 6	Contaminated magma 2 7	Dovyren parental magma 8
SiO_2 (wt%)	45.96	62.80	66.00			53.72	56.72	49.82
TiO_2	0.18	0.50 [a]	0.50			0.50	0.50	0.49
Al_2O_3	4.06	18.90	15.20			14.36	13.45	15.84
FeO_t	7.54	6.50	4.50			9.46	8.05	6.65
MgO	37.78	2.20	2.20			10.62	9.19	7.75
CaO	3.21	1.30	4.20			7.68	7.91	10.00
Na_2O	0.33	1.20	3.90			1.07	2.32	2.08
K_2O	0.03	3.70	3.40	0.31	0.34	1.29	1.56	1.18
mg #	0.899	0.377	0.466			0.667	0.671	0.675
Rb (ppm)	0.535	160	112	0.23	0.33	55.7	51.7	38.3
La	0.614	38	30	0.31	0.40	14.1	14.6	12.9 [b]
Nd	1.19	32	26	0.43	0.55	13.2	13.7	15.8
Sm	0.387	5.6	4.5	0.45	0.60	2.64	2.64	3.15
Eu	0.146	1.67 [a]	1.34 [a]	0.35	0.48	0.85	0.84	0.86 [b]
Yb	0.414	2.8	2.20	0.30	0.48	1.75	1.65	1.68 [b]
Mean				$\overline{0.342}$	$\overline{0.454}$			
Sr	52	200	350			103		271
Sr [c]	52	692 [c]				271	271	
Pb	0.175	20	20			7.2	9.3	
Sm/Nd	0.325	0.175	0.173			0.200	0.193	0.199

(1) Primitive low-Ti picritic basalt, produced by 35% mantle melting (from Arndt et al., 1993).
(2) PAAS is the average post-Archean Australian shale (Taylor and McLennan, 1985).
(3) Average upper continental crust from Taylor and McLennan (1985).
(4) Proportion of mixing between the primitive basalt (column 1) and the PAAS (column 2), required to reproduce the concentrations of incompatible elements in the Dovyren parental magma (column 8).
(5) Proportion of mixing between the primitive basalt (column 1) and the average upper continental crust (column 3), required to reproduce the concentrations of incompatible elements in the Dovyren parental magma (column 8).
(6) Mixture of 65.8% of the primitive basalt (column 1) and 34.2% of PAAS (column 2).
(7) Mixture of 54.6% of the primitive basalt (column 1) and 45.4% of average upper continental crust (column 3).
[a] TiO_2 content in the continental upper crust is also used in the model with PAAS contaminant composition. Eu contents in PAAS and upper crust are adjusted to yield $Eu^*/Eu = 1$, required by nearly zero Eu anomalies in the Dovyren sill samples.
[b] La, Eu and Yb concentrations in the Dovyren parental magma are the means of the sill samples D-2 and TST-24. Other trace-element and major-element concentrations in the Dovyren parental magma are from Table 4. Pb concentrations in the Dovyren rocks were not determined. The Pb concentration in the magma is estimated (very imprecisely) from the Pb concentration in plagioclase (Table 3) and the partition coefficient $D_{Pb}^{(Pl/Liq)} = 0.10–0.14$ (Leeman, 1979) to be 2.5–3.7 ppm.
[c] Sr content in a contaminant, required to reproduce the Sr concentration in the mixture of 271 ppm at the mass fraction of contaminant of 34.2%.

the Dovyren rocks and the estimated chemical composition of the magma are likely to be representative for the magma before emplacement.

5.4. Magma contamination before emplacement or an enriched source?

Because contamination in the magma chamber is shown to have been a process of minor significance, we have to consider pre-emplacement contamination and magma genesis form an enriched mantle source as possible causes of the enriched isotopic signatures in the Dovyren intrusion. In these cases, the country rocks are not a probable contaminant. The isotopic signature of contaminant is thus unknown, and this fact precludes the use of isotopic relationships for the evaluation of a contamination mechanism and mixing proportions. We have instead attempted to use the concentrations of strongly to moderately incompatible elements (Rb, K, Sr, REE and Ti) to constrain the mixing mechanism, and then to use the inferred mixing relationships to calculate the isotopic signature of a contaminant.

Two alternative petrologic models are tested to explain magmatic and contamination processes in the Dovyren intrusion: (1) contamination of a primary magma with or without crystal fractionation; and (2) melting of an enriched mantle source. Overall, the Dovyren intrusion has many chemical similarities to low-Ti basaltic series. We therefore examined the model of a steady-state liquid formation in periodically replenished and tapped magma chamber with continuous fractionation and wallrock assimilation [the RTFA model of O'Hara (1977)]. This model has been successfully used to reproduce major- and trace-element signatures in low-Ti basalts of the Siberian flood basalt province (Wooden et al., 1993) and in Tasmanian dolerites, Australia (Arndt et al., 1993). The proposed Dovyren parental magma has chemical signatures [LILE–LREE enrichment and HFSE (high field strength element) depletion] similar to those of low-Ti basalts in both of these provinces, although more extreme. For the modeling purpose, trace-element concentrations in the primary magma were taken as in the low-Ti picritic basalt, used in the calculations of Arndt et al. (1993) as a primary magma for low-Ti continental flood basalts. Similar concentrations of incompatible elements in the primary magma were calculated with the method of separation of components in a MORB-normalized trace-element pattern (Pearce, 1983), using Ti and Yb concentrations in the suggested Dovyren parental magma as background values. Average upper continental crust and average PAAS from Taylor and McLennan (1985) were taken as contaminants, assuming similar $TiO_2 = 0.5$ wt%. Accumulating assemblage was assumed to be either dunite (100% Ol) or troctolite (75% Ol + 25% Pl), but the difference between these two types of cumulates is significant only for Sr. Using these parameters, we were unable to reproduce the concentrations of Ti and Yb in the Dovyren parental magma within the entire range of parameter q (fraction of total cumulate precipitated to provide energy for wallrock digestion) from 0 to 1, unless unrealistically high bulk partition coefficients ($D > 1$) were assumed for these elements. A similar problem is encountered when using the AFC formalization of Aitcheson and Forrest (1994). Indeed, the concentration of $TiO_2 = 0.5\%$ is similar in the primary basalt and in the contaminant (upper crust), and any fractionation process with bulk $D < 1$ for an accumulating mineral assemblage would increase the TiO_2 concentration in the residual melt above this value.

To overcome the problem of Ti and Yb balance, we tried a simple mixing model without fractionation, using the same end-member compositions. Proportions of mixing, required to reproduce the concentrations in the Dovyren parental magma, were calculated for 7 elements (K, Rb, La, Nd, Sm, Eu, Yb), and the average values were applied to calculate the concentrations of major elements, Sr and Pb in contaminated basalt (Table 5, column 6). Given the large uncertainty in major-element contents in the Dovyren parental magma, the fit between observed and calculated values may be considered reasonable, although the calculated magmas have higher SiO_2, MgO and FeO, and lower CaO and Al_2O_3 than the Dovyren parental magma. Strontium concentrations in the average upper crust and PAAS are too low to reproduce the calculated Sr concentration in the Dovyren parental magma using mixing models (both simple mixing and RTFA). The Sr concentration in a contaminant, estimated from inferred mixing proportions, is ~ 700 ppm (Table 5): 3.5 times higher, than in PAAS, and twice higher, than in average upper

Table 6
Models of mantle source contamination and melting

	Primitive mantle	Depleted lherzolite	PAAS	Lamproite	Mixed source 1	Mixed source 2	Mixed source 3	Melt 1	Melt 2	Melt 3	Dovyren parental magma
Column	1	2	3	4	5	6	7	8	9	10	11
SiO_2 (wt%)	45.96	44.95	62.80	53.30	46.85	46.56	45.18	46.82	49.82	49.82	49.82
TiO_2	0.18	0.08	0.50 [a]	3.00	0.20	0.12	0.16	0.99	0.45	0.65	0.49
Al_2O_3	4.06	3.22	18.90	9.10	4.85	4.63	3.38	24.23	17.81	13.54	15.84
FeO_t	7.54	7.66	6.50	6.30	7.48	7.56	7.62	2.00	6.73	8.50	6.65
MgO	37.78	40.03	2.20	12.10	35.89	36.63	39.25	2.33	7.83	9.90	7.75
CaO	3.21	2.99	1.30	5.80	3.11	2.84	3.07	15.54	10.92	12.27	10.00
Na_2O	0.33	0.18	1.20	1.40	0.38	0.27	0.21	1.89	1.05	0.86	2.08
K_2O	0.03	0.02	3.70	7.20	0.23	0.35	0.22	1.13	1.35	0.88	1.18
mg #	0.899	0.645	0.377	0.774	0.895	0.896	0.902	0.675	0.675	0.675	0.675
Rb (ppm)	0.535	0.02	160	272	8.99	14.4	7.64	44.9	55.4	30.5	38.3
La	0.614	0.03	38	240	2.60	3.45	6.45	13.0	13.3	27.0	12.9 [b]
Sr	18.21	0.80	200	1530	27.8	18.73	43.6	139	72.0	174	271
Sr [c]	18.21	0.80	692 [c]		53.9	63.0		270	242		271
Nd	1.19	0.133	32	207	2.82	3.00	5.93	14.1	11.5	23.7	15.8
Pb	0.175	0.006 [d]	20	60 [e]	1.23	1.81	1.69	6.13	6.94	6.74	7.2 [b]
Sm	0.387	0.101	5.6	24	0.66	0.60	0.77	5.45	2.29	3.08	3.15
Eu	0.146	0.050	1.67 [a]	4.8	0.23	0.20	0.18	1.13	0.75	0.73	0.86 [b]
Yb	0.414	0.269	2.8	1.7	0.54	0.50	0.31	2.7	1.91	1.24	1.68 [b]
Sm/Nd	0.325	0.759	0.175	0.116	0.235	0.199	0.130	0.235	0.199	0.130	0.199

(1) Primitive mantle composition from Hofmann (1988).
(2) Depleted lherzolite is a spinel lherzolite (Tinaquillo peridotite; Jaques and Green, 1980), more refractory than the primitive mantle. The major-element concentrations are from Jaques and Green (1980), and are similar to average spinel lherzolite (Maaløe and Aoki, 1977; McDonough, 1990). Concentrations of incompatible trace elements are from Philpotts et al. (1972), and are lower than in average spinel lherzolite (McDonough, 1990).
(3) PAAS is the average post-Archean Australian shale (Taylor and McLennan, 1985).
(4) Average lamprotie composition is from Bergman (1987).
(5) Mixture of 94.7% primitive mantle (column 1) and 5.3% PAAS (column 3).
(6) Mixture of 91% depleted lherzolite (column 2) and 9% PAAS (column 3).
(7) Mixture of 97.2% depleted lherzolite (column 2) and 2.8% lamproite (column 4).
(8) Composition of the mixed source 1 (column 5) after subtraction of 80% of residual harzburgite (65% $Ol_{Fo\ 86}$ and 14% $Opx_{En\ 90}$). Composition of Ol is chosen to yield mg # = 0.675 in the melt, similar to the calculated value in the Dovyren parental magma. It is assumed that all components except SiO_2, MgO and FeO concentrate entirely in the melt.
(9) Composition of the mixed source 2 (column 6) after subtraction of 74% residue (75% $Ol_{Fo\ 88.4}$ and 25% $Opx_{En\ 90}$). Composition of Ol is chosen to yield mg # = 0.675 in the melt. Ol/Opx ratio in the residue is chosen to yield the SiO_2 = 49.82 wt% in the melt (similar to the Dovyren parental magma).
(10) Composition of the mixed source 3 (column 7) after subtraction of 75% residue (86% $Ol_{Fo\ 89.5}$ and 14% $Opx_{En\ 90}$). Composition of Ol is chosen to yield mg # = 0.675 in the melt. Ol/Opx ratio in the residue is chosen to yield the SiO_2 = 49.82 wt% in the melt.
[a] TiO_2 content in the continental upper crust (Taylor and McLennan, 1985). Eu content is adjusted to yield $Eu^*/Eu = 1$, required by nearly zero Eu anomalies in the Dovyren sill samples.
[b] La, Eu and Yb concentrations in the Dovyren parental magma are the means of the sill samples D-2 and TST-24. Pb content in the magma is estimated from mixing proportions in the magma contamination model (Table 5). Other trace- and major-element contents in the Dovyren parental magma are from Table 4.
[c] Sr concentration in the contaminant, estimated from mixing proportions in the magma contamination model (Table 5).
[d] Pb content in the Tinaquillo peridotite is not given by Philpotts et al. (1972). Estimated from N-MORB-normalized abundances of LREE, having similar incompatibility with Pb (Sun and McDonough, 1989).
[e] Pb content in lamproite is the mean of lamproite analyses from Nelson et al. (1986).

crust, but lower than Sr concentration of 1000 ppm in contaminant, used by Wooden et al. (1993) in their RTFA calculations. A problem with the model of bulk assimilation of a crustal material by picritic basalt is a very high mass fraction of contaminant of 34% for PAAS or 45% for average upper crust, considerably higher than the maximum amounts of contamination for picritic basalt during magma ascent estimated by Huppert and Sparks (1985).

All the problems with the bulk assimilation and assimilation + fractionation models mentioned above also exist if contaminant had lower-crustal composition (Taylor and McLennan, 1985; Halliday et al., 1993). The lower concentrations of incompatible elements in lower-crustal rocks would require unreasonably high proportions of contaminant. In addition, lower-crustal contamination cannot account for the high K and Rb concentrations and LILE/LREE ratios in the Dovyren parental magma. Because of these reasons, we do not consider lower crust as a likely contaminant.

An alternative to the magma contamination is the possibility that the mantle source of the Dovyren magmas had been modified by the addition of sedimentary material in a subduction zone environment. This model was used by Hergt et al. (1989), Hergt et

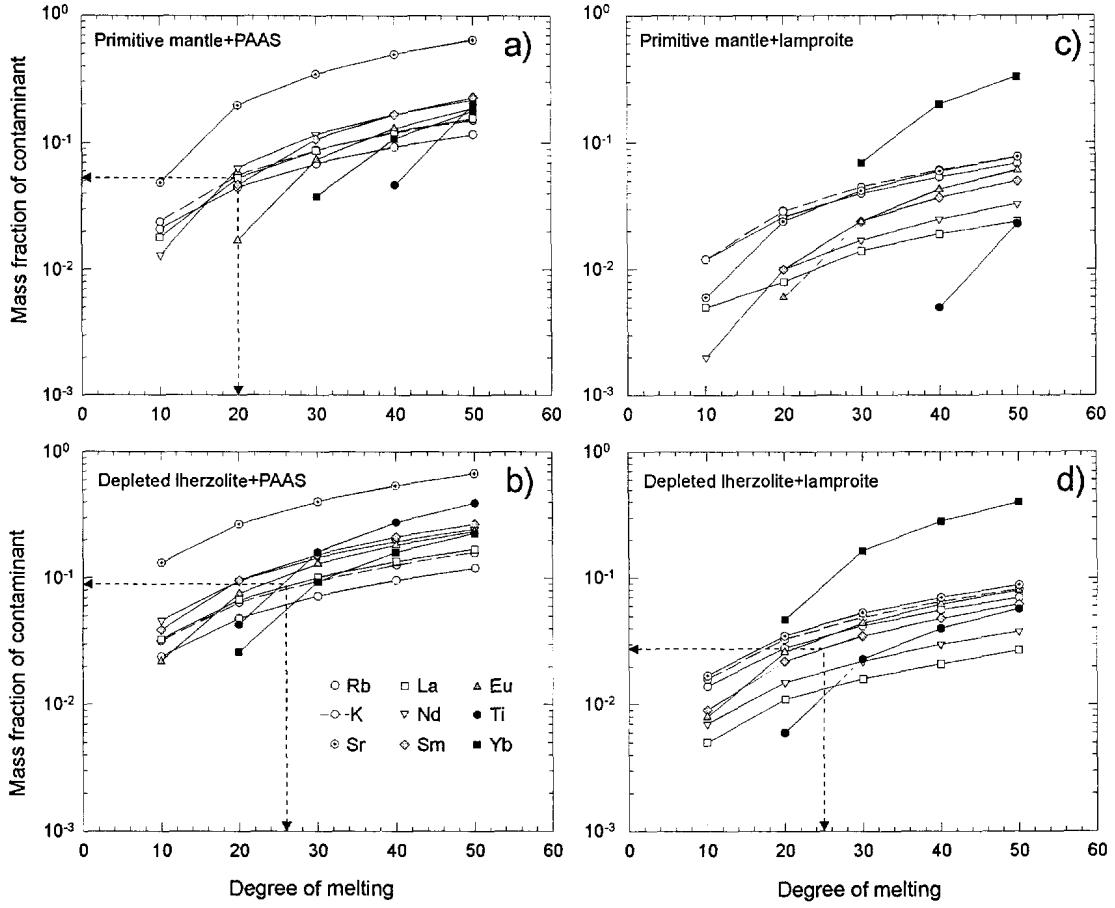

Fig. 12. Diagrams showing proportions of mixing and corresponding degrees of melting, required by the source contamination models to reproduce concentrations of strongly to moderately incompatible elements in the Dovyren parental magma. The concentrations of incompatible elements in mixing end-members are given in Table 6. The probable mixing proportions, shown by *dashed arrows*, were estimated as the means of mixing proportions for different elements, by varying the degree of melting to yield the minimum scatter of mixing proportions, calculated for different elements. Specific comments: (a, b) Sr is not included in mixing proportion estimates in the models using PAAS as a contaminant; (a) minimum scatter estimate is for 5 elements only (K, Rb, La, Nd, Sm).

al. (1991) and Lightfoot et al. (1993) to explain LILE–LREE enrichment, HFSE depletion, and crust-like isotopic signatures in low-Ti continental flood basalts from Tasmania and Siberia. As mentioned above, the suggested Dovyren parental magma has similar chemical features. Mixing calculations (Table 6; Fig. 12b) show a relatively good consistency between mixing proportions for K, Rb, REE and Ti, when the end-members are depleted lherzolite and PAAS. Good agreement can also be achieved with primitive mantle and PAAS (Fig. 12a), but only at an unrealistically high degree of melting (~ 50%). Models using lamproite as a contaminant (Ellam and Cox, 1991) do not yield good agreement (Fig. 12c

Table 7
Estimated Sr-, Nd- and Pb-isotopic compositions (673 Ma) of an enriched component in the magma contamination and mantle source contamination models

	Mixture (Dovyren)	Depleted end-member [a]	% of element from enriched end-member [2)]	Estimated enriched end-member	$T_{Nd}(DM)$ [c] (Ga)
(1) Primitive picritic basalt + PAAS *(0.66 + 0.34)*:					
$^{87}Sr/^{86}Sr$	0.7103	0.7027	87	0.7116	
$^{87}Sr/^{86}Sr$	0.7135	0.7027	87	0.7153	
ε_{Nd}	−14.8	+7.2	83	−20.5	2.75
$^{206}Pb/^{204}Pb$	16.90	17.00	95	16.89	
$^{207}Pb/^{204}Pb$	15.48	15.35	95	15.49	
$^{208}Pb/^{204}Pb$	37.50	36.80	95	37.54	
(2) Primitive mantle + PAAS *(0.947 + 0.053); 20% melting*:					
$^{87}Sr/^{86}Sr$	0.7103	0.7027	68	0.7169	
$^{87}Sr/^{86}Sr$	0.7135	0.7027	68	0.7229	
ε_{Nd}	−14.8	+7.2	64	−42.0	4.26
$^{206}Pb/^{204}Pb$	16.90	17.00	89	16.89	
$^{207}Pb/^{204}Pb$	15.48	15.35	89	15.50	
$^{208}Pb/^{204}Pb$	37.50	36.80	89	37.60	
(3) Depleted lherzolite + PAAS *(0.91 + 0.09); 26% melting*:					
$^{87}Sr/^{86}Sr$	0.7103	0.7027	98.9	0.7104	
$^{87}Sr/^{86}Sr$	0.7135	0.7027	98.9	0.7136	
ε_{Nd}	−14.8	+7.2	96.9	−15.5	2.39
$^{206}Pb/^{204}Pb$	16.90	17.00	99.0	16.90	
$^{207}Pb/^{204}Pb$	15.48	15.35	99.0	15.48	
$^{208}Pb/^{204}Pb$	37.50	36.80	99.0	37.51	
(4) Depleted lherzolite + lamproite (0.972 + .028); 25% melting:					
$^{87}Sr/^{86}Sr$	0.7103	0.7027	98.9	0.7104	
$^{87}Sr/^{86}Sr$	0.7135	0.7027	98.9	0.7136	
ε_{Nd}	−14.8	+7.2	96.7	−15.6	1.97
$^{206}Pb/^{204}Pb$	16.90	17.00	98.9	16.90	
$^{207}Pb/^{204}Pb$	15.48	15.35	98.9	15.48	
$^{208}Pb/^{204}Pb$	37.50	36.80	98.9	37.51	

[a] Isotopic compositions of the depleted end-member are those of the 630-Ma Chaya gabbronorite–peridotote massif in the Baikal–Muya ophiolite belt. These compositions are close to the depleted mantle model values (e.g., Zartman and Haines, 1988).
[b] Contributions from the enriched component (contaminant) are calculated from concentrations of Sr, Nd and Pb in depleted and enriched components (Tables 5 and 6) and mixing proportions shown in these tables.
[c] Single-stage model ages, calculated relative to the linear model for the depleted mantle (Goldstein and Jacobsen, 1988), using Sm/Nd ratios in contaminants (PAAS and lamproite).

and d), because they fail to reproduce the REE distribution in the Dovyren parental magma. To calculate the major-element contents in melts derived from contaminated mantle sources, we have used the evaluated mixing proportions together with appropriate degrees of melting (Fig. 12). Calculated major-element concentrations in a hypothetical melt, derived from the mixture of depleted lherzolite + PAAS (column 9 in Table 6), are in close agreement (except Na) with the composition of the Dovyren parental magma.

The models discussed above rely on the estimate of the Dovyren parental magma composition, which is, in turn, based on the composition of the most magnesian olivine. Compositions of olivine in zone-*A* dunites and the olivine inclusions in chromite are in good agreement, but there is still a possibility that both olivines were equilibrated with the magma before the crystallization of chromite. If this were the case, then the parental magma was more magnesian than we have estimated. Taking MgO = 15.7 wt% in the primary magma from Papunen et al. (1992) and using the same correlations of major- and trace-element concentrations with MgO as above, we can calculate an alternative, more primitive, magma composition, shown in Table 4 (column 9). The concentrations of K, Ti, REE, Rb and Sr are 1.3 times lower than in the hypothetical parental magma with 7.75 wt% MgO. The parental magma composition with 15.7 wt% MgO cannot be produced in the model of magma contamination starting with picritic basalt, and requires komatiite as a primary magma. The model of the source contamination can reproduce the major- and trace-element concentrations in the parental magma with 15.7 wt% MgO at 35% melting of a source, containing 91 wt% depleted peridotite and 9 wt% PAAS. The fact that the proportion of mixing in the source contamination model is essentially independent of magma composition and the inferred degree of melting is a result of mass

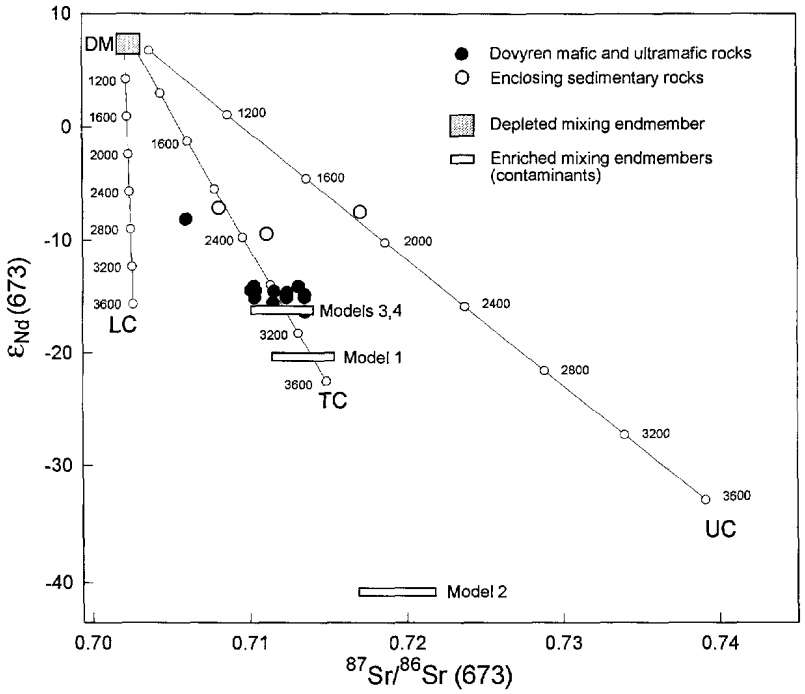

Fig. 13. ε_{Nd}(673 Ma) vs. $^{87}Sr/^{86}Sr$(673 Ma) plot for the Dovyren mafic and ultramafic rocks and host metasediments, and depleted and enriched mixing end-member isotopic compositions (from Table 7). Numbers of mixing models are as in Table 7. Shown for comparison are evolution paths of lower (*LC*), total (*TC*) and upper (*UC*) continental crust with Sm/Nd ratios of 0.249, 0.219 and 0.173, and Rb/Sr ratios of 0.023, 0.123 and 0.320, respectively, after Taylor and McLennan (1985). Labels on the crust evolution lines correspond to the time (Ma before present) of separation of a crust from a depleted mantle [linear model after Goldstein and Jacobsen (1988)].

balance of incompatible elements, controlled almost entirely by the contaminant.

5.5. Speculation about the isotopic signatures of a contaminant

At given isotopic compositions of a depleted end-member and the mixture (the Dovyren values), the isotopic signature of an enriched end-member is the function of the mixing proportion, expressed as the fraction of the element in question (Sr, Nd, Pb), provided by the enriched component. Isotopic compositions of a contaminant, calculated in models where almost all Sr, Nd and Pb are contributed by the enriched component (depleted lherzolite + PAAS and depleted lherzolite + lamproite) are nearly identical to the initial values in the Dovyren intrusion (Table 7; Fig. 13). The highest $^{87}Sr/^{86}Sr$ and the lowest ε_{Nd} were calculated using the primitive mantle + PAAS source contamination model. The $\varepsilon_{Nd} = -42$ corresponds to the model age of > 4 Ga (using Sm/Nd in the PAAS and either DM or CHUR as a reference), and seems therefore unreasonably low. More realistic Sm–Nd model ages of 2.4–2.8 Ga (relative to DM) were calculated in the depleted lherzolite + PAAS model (#3, Table 7) and in the picritic basalt contamination model (#1, Table 7). The latter models are preferred on geochemical grounds, and we therefore consider 2.4–2.8 Ga as the probable age of the enriched component (an average residence age of the crust assimilated by picritic basalt, or the protolith age of subducted sediments).

Additional constraints on the history of the contaminant, almost independent on the choice of the model, can be inferred from the Pb-isotopic data. It is noteworthy that Pb-isotopic compositions of contaminants are nearly identical in all models and are very close to the measured Dovyren values, due to low Pb concentrations in depleted end-members. High $^{207}Pb/^{204}Pb$ at a given $^{206}Pb/^{204}Pb$ and enhanced $^{208}Pb/^{204}Pb$ (and, therefore, high time-integrated Th/U) require a two-stage (or more complex) history of the U–Pb system: earlier stage with high μ_1, and later stage with lower μ_2 and high Th/U. With a two-stage Pb evolution model, starting from the depleted mantle (Neymark, 1990) at 2.4–2.8 Ga, we can calculate the minimum age of U depletion at 1.23–1.24 Ga, with $\mu_2 = 0$ (at younger age of U depletion μ_2 becomes negative). If U–Pb fractionation occurred at 1.5–2.0 Ga, then the values $\mu_1 = 11–12$ and $\mu_2 = 4.2–6.3$ can be calculated, which are close to the average μ-values for upper continental crust (Zartman and Haines, 1988) and pelagic sediments (Ben Othman et al., 1989), respectively. These μ-values are consistent with the model of U depletion during erosion of 2.4–2.8-Ga upper continental crust and sediment subduction at 1.5–2.0 Ga.

Integrated major- and trace-element and isotopic data suggest that subduction-related enrichment of a depleted mantle lherzolite, involving sediments derived from ancient ($\sim$ 2.4–2.8 Ga) upper continental crust, is a plausible model for the origin of the Dovyren parental magma. An important feature of this model, as well as of the model of magma contamination, is a very high proportion of contaminant. The amount of subducted sediment in the source contamination model (9%) is higher than 3–5%, calculated in similar models for low-Ti continental flood basalts (Hergt et al., 1989, 1991; Lightfoot et al., 1993), and may seem unreasonably high. However, the evidence for the existence of strongly metasomatized mantle regions suggests that the mantle source contamination model may be real. This evidence is provided by the occurrence of peridotite xenoliths with abundant mica and/or K-richterite and K, Rb, Sr and REE concentrations similar to, or higher than, our hypothetical contaminated mantle source, and retaining ancient enriched isotopic signatures (Kramers et al., 1983; Hawkesworth et al., 1990; Carlson and Irving, 1994).

Recent geochronological, geochemical and isotopic data for the North Baikal volcano-plutonic belt (Fig. 1) provide some evidence for ancient subduction in the Baikal fold area and for the existence of an enriched mantle domain — a possible source of the Dovyren magmas — beneath the Siberian Plate since the early Proterozoic (Neymark et al., 1996). The 2020–2060-Ma granitoids with volcanic arc geochemical affinity are identified within the belt, as well as early Proterozoic granitoids and bimodal volcanics having within-plate affinity and negative ε_{Nd}-values. The 1850-Ma continental basalts in the belt demonstrate the range of initial ε_{Nd}(1850 Ma)-values from -6.1 to -4.6, which corresponds to the

range of ε_{Nd} from −18.4 to −17.7 in their source at the time of the Dovyren emplacement. If this mantle domain still existed during the late Proterozoic, it could have been a source (or a component of the source) for the parental magmas of the Dovyren intrusion.

6. Conclusions

Geochemical and Nd-, Pb- and Sr-isotopic features of the layered series and marginal rocks of the 673-Ma Dovyren intrusion and associated mafic sills, indicate that late Archean–early Proterozoic upper continental crustal material was extensively involved in the generation of the parental basaltic magmas of the intrusion. However, these features are not the result of contamination in the magma chamber. They could rather be the result of either contamination of primitive high-Mg, low-Ti picritic basalt by sedimentary or granitic basement material, or, more likely, subduction of continent-derived sediments into depleted mantle. A model of magma contamination suggests that a large amount (~ 34–45%) of a crustal component was assimilated by a depleted mantle primary melt. In the model of depleted mantle source contamination, the mixing proportion of a subducted sediment, calculated from the mass-balance relations for K, Rb, REE and Ti, is ~ 9%. In both models, the estimated proportions of enriched component are rather high, but probably not unreasonable. A simple model of the contamination of depleted lherzolite by PAAS with subsequent partial melting, leaving a harzburgitic residue, gives a close fit with the major-element composition of the Dovyren parental magma. Initial Nd- and Pb-isotopic compositions of the Dovyren intrusion suggest that the contaminant was probably derived from 2.4–2.8-Ga upper continental crust and underwent U depletion at 1.5–2.0 Ga.

Acknowledgements

We gratefully acknowledge G.V. Ovchinnikova and B.M. Gorokhovsky for support in Pb-isotope analytical work, E.V. Koptev-Dvornikov for providing samples, and I.K. Shuleshko and group for completing mineral separations. We thank R.T. Pidgeon, I.R. Fletcher, D.R. Nelson, L.M. Heaman, F. Corfu and D. Unruh for helpful criticism on earlier versions of the manuscript, and C. Mitchell, A.C. Kerr, D.A. Ionov, D.L. Nealey and N.T. Arndt for thoughtful reviews. This work was supported by grant of the Russian Academy of Sciences for advanced research.

References

Aitcheson, S.J. and Forrest, A.H., 1994. Quantification of crustal contamination in open magmatic systems. J. Petrol., 35: 461–488.

Amelin, Yu.V. and Neymark, L.A., 1995.Pb isotope geochemistry of early Proterozoic layered intrusions in the eastern Baltic Shield. Int. Proc. Symp. Petrology and Metallogeny of Volcanic and Intrusive Rocks of the Midcontinent rift System. Duluth, MN, pp. 5–6.

Arndt, N.T., Czamanske, G.K., Wooden, J.L. and Fedorenko, V.A., 1993. Mantle and crustal contributions to continental flood volcanism. Tectonophysics, 223: 39–52.

Barnes, S.J., 1986. The effect of trapped liquid crystallization on cumulus mineral compositions in layered imtrusions. Contrib. Mineral. Petrol., 93: 524–531.

Ben Othman, D., White, W.M. and Patchett, J., 1989. The geochemistry of marine sediments, island arc magma genesis, and crust–mantle recycling. Earth Planet. Sci. Lett., 94: 1–21.

Bergman, S.C., 1987. Lamproites and other potassium-rich igneous rocks: a review of their occurrence, mineralogy and geochemistry. In: F.J. Fitton and B.G.J. Upton (Editors), Alkaline Igneous Rocks. Geol. Soc. London, Spec. Publ., 30: 103–190.

Carlson, R.W. and Irving, A.J., 1994. Depletion and enrichment history of subcontinental lithospheric mantle: An Os, Sr, Nd and Pb isotopic study of ultramafic xenoliths from the northwestern Wyoming Craton. Earth Planet. Sci. Lett., 126: 457–472.

Chai, G. and Naldrett, A.J., 1992. The Jinchuan ultramafic intrusion: cumulate of a high-Mg basaltic magma. J. Petrol., 33: 277–303.

Chalokwu, C.I. and Grant, N.K., 1987. Reequilibration of olivine with trapped liquid in the Duluth complex, Minnesota. Geology, 19: 71–74.

Cox, K.G. and Hawkesworth, C.J., 1985. Geochemical stratigraphy of the Deccan traps at Mahabaleshwar, Western Ghats, India, with implications for open system magmatic processes. J. Petrol., 26: 355–377.

DePaolo, D.J., 1981. Trace element and isotopic effects of combined wallrock assimilation and fractional crystallization. Earth Planet. Sci. Lett., 52: 177–184.

DePaolo, D.J., 1985. Isotopic studies of processes in mafic magma chambers, I. The Kiglapait intrusion, Labrador. J. Petrol., 26: 925–951.

DePaolo, D.J. and Wasserburg, G.J., 1976. Nd isotopic variations and petrogenetic models. Geophys. Res. Lett., 3: 249–252.

Ellam, R.M. and Cox, K.G., 1991. An interpretation of Karoo picrite basalts in terms of interaction between asthenospheric magmas and the mantle lithosphere. Earth Planet. Sci. Lett., 105: 330–342.

Gerling, E.K., Koltsova, T.V., Matveeva, I.I., Shukolyukov, Y.A. and Yakovleva, S.Z., 1962. Dating of mafic rocks by the K–Ar method. Geokhimiya, 11: 1055–1062.

Goldstein, S.J. and Jacobsen, S.B., 1988. Nd and Sr isotopic systematics of river water suspended material: Implications for crustal evolution. Earth Planet. Sci. Lett., 87: 249–265.

Gray, C.M., Cliff, R.A. and Groode, A.D., 1981. Neodymium–strontium isotope evidence for extreme contamination in a layered basic intrusion. Earth Planet. Sci. Lett., 56: 189–198.

Gurulev, S.A., 1965. The Geology and Conditions of Formation of the Yoko-Dovyren Gabbro-peridotite Intrusion. Nauka, Moscow (in Russian).

Gurulev, S.A., 1983. Conditions of Formation of Basic Layered Intrusions. Nauka, Moscow, 249 pp. (in Russian)

Halliday, A.N., Dickin, A.P., Hunter, R.N., Davies, G.R., Dempster, T.J., Hamilton, P.J. and Upton, B.G.J., 1993. Formation and composition of the lower continental crust: evidence from Scottish xenolith suites. J. Geophys. Res., 98: 581–607.

Hawkesworth, C.J., March, J.S., Duncan, A.R., Erlank, A.J. and Norry M.J., 1984. The role of continental lithosphere in the generation of the Karoo volcanic rocks: evidence from combined Nd- and Sr-isotopic studies. Spec. Publ. Geol. Soc. S. Afr., 13: 341–354.

Hawkesworth, C.J., Erlank, A.J., Kempton, P.D. and Waters, F.G., 1990. Mantle metasomatism: Isotope and trace-element trends in xenoliths from Kimberley, South Africa. Chem. Geol., 85: 19–34.

Heaman, L.M. and Machado, N., 1992. Timing and origin of Midcontinent rift alkaline magmatism, North America: evidence from the Coldwell Complex. Contrib. Mineral. Petrol., 110: 289–303.

Hergt, J.M., Chappell, B.W., McCulloch, M.T., McDougall, I. and Chivas, A.R., 1989. Geochemical and isotopic constraints on the origin of the Jurassic dolerites of Tasmania. J. Petrol., 30: 841–883.

Hergt, J.M., Peate, D.W. and Hawkesworth, C.J., 1991. The petrogenesis of Mesozoic Gondwana low-Ti flood basalts. Earth Planet. Sci. Lett., 105: 134–148.

Hofmann, A.W., 1988. Chemical differentiation of the Earth: the relationship between mantle, continental crust, and oceanic crust. Earth Planet. Sci. Lett., 90: 297–314.

Huppert, H.E. and Sparks, R.S.J., 1985. Cooling and contamination of mafic and ultramafic magmas during ascent through continental crust. Earth Planet. Sci. Lett., 74: 371–386.

Ionov, D.A., Abramov, A.V. and Yaroshevsky, A.A, 1984a. Geochemistry of rock-forming minerals in the Ioko-Dovyren layered intrusion. Geochem. Int., 21(2): 123–140.

Ionov, D.A., Abramov, A.V. and Yaroshevsky, A.A., 1984b. Geochemical features of the structure of the Ioko-Dovyren layered intrusion. Geochem. Int., 21(3): 85–92.

Jacobsen, S.B. and Wasserburg, G.J., 1980. Sm–Nd evolution of chondrites. Earth Planet. Sci. Lett., 50: 139–155.

Jaques, A.L. and Green, D.H., 1980. Anhydrous melting of peridotite at 0–15 Kb pressure and the genesis of tholeiitic basalts. Contrib. Mineral. Petrol., 73: 297–310.

Kelemen, P.B., Dick, H.J.B. and Quick, J.E., 1992. Formation of harzburgite by pervasive melt/rock reaction in the upper mantle. Nature (London), 358: 635–641.

Kelemen, P.B., Shimizu, N. and Salters, V.J.M., 1995. Extraction of mid-ocean-ridge basalt from the upwelling mantle by focused flow of melt in dunite channels. Nature (London), 358: 635–641.

Kislov, E.V., 1990. Silicate inclusions in chrome-spinels of endocontact dunites of the Ioko-Dovyren Massif. Sov. Geol. Geophys., 31(10): 43–46.

Kislov, E.V., Konnikov, E.G., Posokhov, V.F. and Shalagin, V.L., 1989. Isotope evidence of crustal contamination in the Ioko-Dovyren Pluton. Sov. Geol. Geophys., 30(9): 126–129.

Konnikov, E.G., Kislov, E.V. and Kacharovskaya, L.N., 1988. New data on the petrology and ore content of the Ioko-Dovyren Massif. Sov. Geol. Geophys., 29(3): 33–41.

Konnikov, E.G., Kacharovskaya, L.N., Zaguzin, G.N. and Postnikova, A.A., 1990. Features of the composition of the main minerals of sulfide ores of the Baikal copper–nickel field. Sov. Geol. Geophys., 31(2): 57–63.

Kramers, J.D., Roddick, J.C.M. and Dawson, J.B., 1983. Trace element and isotope studied of veined, metasomatic and "MARID" xenoliths from Bultfontein, South Africa. Earth Planet. Sci. Lett., 65: 90–106.

Krivopliasov, G.S., Yaroshevsky, A.A., Ustinov, V.I. and Strizhov, V.P., 1982. Redistribution of oxygen isotopes during the interaction of magmatic system with enclosing rocks (based on example of Ioko-Dovyren massif, North Baikal region). 9th All-Union Symp. on Stable Isotope Geochemistry, Moscow (abstract, in Russian).

Krivopliasov, G.S., Yaroshevsky, A.A. and Ustinov, V.I., 1984. Oxygen isotope composition in rock-forming minerals of some differentiated trapp sills and in a major layered intrusion (on example of trapps of Norilsk region and Ioko-Dovyren massif). 10th All-Union Symp. on Stable Isotope Geochemistry, Moscow (abstract, in Russian).

Lambert, D.D., Morgan, J.W., Walker, R.J., Shirey, S.B., Carlson, R.W., Zientek, M.L. and Koski, M.S., 1989. Rhenium–osmium and samarium–neodymium isotopic systematics of the Stillwater Complex. Science, 224: 1169–1174.

Lambert, D.D., Walker, R.J., Morgan, J.W., Shirey, S.B., Carlson, R.W., Zientek, M.L., Lipin, B.R., Koski, M.S. and Cooper, R.L., 1994. Re–Os and Sm–Nd isotope geochemistry of the Stillwater Complex, Montana: implications for the petrogenesis of the J-M Reef. J. Petrol., 35: 1717–1753.

Leeman, W.P., 1979. Partitioning of Pb between volcanic glass and coexisting sanidine and plagioclase feldspars. Geochim. Cosmochim. Acta, 43: 171–175.

Lightfoot, P.C., Hawkesworth, C.J., Hergt, J., Naldrett, A.J., Gorbachev, N.S., Fedorenko, V.A. and Doherty, W., 1993. Remobilisation of the continental lithosphere by a mantle plume: major-, trace-element, and Sr-, Nd-, and Pb-isotope evidence from picritic and tholeiitic lavas of the Noril'sk District, Siberian Trap, Russia. Contrib. Mineral. Petrol., 114: 171–188.

Ludwig, K.R., 1992. Isoplot — a plotting and regression program for radiogenic isotope data, for IBM-PC compatible computers, version 2.57. U.S. Geol. Surv., Open-File Rep. 91-445, 40 pp.

Maaløe, S. and Aoki, K.I., 1977. The major element composition of the upper mantle estimated from the composition of lherzolites. Contrib. Mineral. Petrol., 63: 161–173.

Manhes, G., Minster, I.E. and Allègre, C.J., 1978. Comparative uranium–thorium–lead and rubidium–strontium study of the Saint Severin amphoterite: consequences for early solar system chronology. Earth Planet. Sci. Lett., 39: 14–24.

McDonough, W.F., 1990. Constraints on the composition of the continental lithospheric mantle. Earth Planet. Sci. Lett., 101: 1–18.

Nelson, D.R., McCulloch, M.T. and Sun, S.-s., 1986. The origins of ultrapotassic rocks as inferred from Sr, Nd and Pb isotopis. Geochim. Cosmochim. Acta, 50: 231–245.

Neymark, L.A., 1987. Potential and restrictions of the lead-isochron method in dating lower Precambrian polymetamorphic rocks. In: Yu.A. Shukolyukov (Editor), Isotopic Dating of Metamorphic and Metasomatic Processes. Nauka, Moscow, pp. 29–44 (in Russian).

Neymark, L.A., 1990. Lead isotopes, $^{Pb}T_{DM}$ parameter and the crustal pre-history of rocks. In: W. Compston (Editor), Seventh International Conference on Geochronology, Cosmochronology and Isotope Geology; Abstracts Volume. Abstr. Geol. Soc. Aust., 27: 70.

Neymark, L.A., Ritsk, E.Yu., Gorokhovsky, B.M., Ovchinnikova, G.V., Kiseleva, E.I. and Konkin, V.D., 1991a. Lead isotopic composition and genesis of Pb–Zn ores in the Olokit zone, North Baikal Region. Geol. Ore Deposits, 33: 34–49 (in Russian).

Neymark, L.A., Larin, A.M., Ritsk, E.Yu., Amelin, Yu.V. and Lapshin, S.G., 1991b. Geodynamic environments for the granitoid magmatism in the Baikal Fold Area: geochemical and isotopic evidence. Int. Symp. on Granites and Geodynamics, Abstr. Vol., Moscow, pp. 77–78.

Neymark, L.A., Larin, A.M., Nemchin, A.A. and Ritsk, E.Yu., 1996. Anorogenic magmatism in the North Baikal volcano-plutonic belt: geochronological, geochemical and isotopic study. Petrology (submitted).

O'Hara, M.J., 1977. Geochemical evolution during fractional crystallisation of a periodically refilled magma chamber. Nature (London), 266: 503–507.

Papunen, H., Distler, V. and Sokolov, A., 1992. PGE in the upper Proterozoic Dovirensky layered complex, North Baikal area, Siberia. Aust. J. Earth Sci., 39: 327–334.

Parsons, I. (Editor), 1986. Origins of Igneous Layering. NATO (N. Atlantic Treaty Org.) ASI (Adv. Stud. Inst.) Ser. C, Vol. 196. D. Reidel, Dordrecht, 666 pp.

Pearce, T.H., 1968. A contribution to the theory of variation diagrams. Contrib. Mineral. Petrol., 19: 142–157.

Pearce, J.A., 1983. Role of sub-continental lithosphere in magma genesis at active continental margins. In: C.J. Hawkesworth and M.J. Norry (Editors), Continental Basalts and Mantle Xenoliths. Shiva, Nantwich, pp. 230–249.

Philpotts, J.A., Schnetzler, C.C. and Thomas, H.H., 1972. Petrogenetic implications of some new geochemical data on eclogitic and ultrabasic inclusions. Geochim. Cosmochim. Acta, 36: 1131–1166.

Poitrasson, F., Pin, C. and Duthou, J-L., 1994. The size-isotopic evolution connection among layered mafic intrusions: Clues from a Sr–Nd isotopic study of a small complex. J. Geophys. Res., 99: 9441–9451.

Premo, W.R., Helz, R.T., Zientek, M.L. and Langston, R.B., 1990. U–Pb and Sm–Nd ages for the Stillwater Complex and its associated sills and dikes, Beartooth Mountains, Montana: Identification of a parental magma? Geology, 18: 1065–1068.

Puchtel, I.S., Zhuravlev, D.Z., Samsonov, A.V. and Arndt, N.T., 1993. Petrology and geochemistry of metamorphosed komatiites and basalts from the Tungurcha greenstone belt, Aldan Shield. Precambrian Res., 62: 399–417.

Richard, P., Shimizu, N. and Allègre, C.J., 1976. $^{143}Nd/^{146}Nd$, a natural tracer: an application to oceanic basalts. Earth Planet. Sci. Lett., 31: 269–278.

Richardson, S.H., 1984. Sr, Nd and O isotope variation in an extensive Karoo dolerite sheet, southern Namibia. Spec. Publ. Geol. Soc. S. Afr., 13: 289–293.

Roeder, P.L. and Emslie, R.F., 1970. Olivine–liquid equilibrium. Contrib. Mineral. Petrol., 29: 275–289.

Salop, L.I., 1967. Geology of the Baikal Highland Area, Vol. 2: Magmatism, Tectonics and History of Geologic Evolution. Nauka, Moscow, 699 pp. (in Russian).

Stacey, J.S. and Kramers, J.D., 1975. Approximation of terrestrial lead isotope evolution by a two-stage model. Earth Planet. Sci. Lett., 26: 207–221.

Stewart, B.W. and DePaolo, D.J., 1990. Isotopic studies of processes in mafic magma chambers, II. The Skærgaard intrusion, East Greenland. Contrib. Mineral. Petrol., 104: 125–141.

Sun, S.-s. and McDonough, W.F., 1989. Chemical and isotopic systematics of oceanic basalts: implications for mantle composition and processes. In: A.D. Saunders and M.J. Norry (Editors), Magmatism in Ocean Basins. Geol. Soc. London, Spec. Publ., 42: 313–345.

Sun, S.-s., Nesbitt, R.W. and Sharaskin, A.Ya., 1979. Geochemical characteristics of mid-ocean ridge basalts. Earth Planet. Sci. Lett., 44: 119–138.

Taylor, S.R. and McLennan, S.M., 1985. The Continental Crust, Its Composition and Evolution. Blackwell, Oxford, 312 pp.

Thirlwall, M.F., 1991. High-precision multicollector isotopic analysis of low levels of Nd as oxide. Chem. Geol. (Isot. Geosci. Sect.), 94: 13–22.

Voshage, H., Hofmann, A.W., Mazzucchelli, M., Rivalenti, G., Sinigoi, S., Raczek, I. and Demarchi, G., 1990. Isotopic evidence from the Ivrea zone for a hybrid lower crust formed by magmatic underplating. Nature (London), 347: 731–736.

Wager, L.R. and Brown, G.M., 1967. Layered Igneous Rocks. Freeman, San Francisco, Calif. and (1968) Oliver & Boyd, London, 588 pp.

Wooden, J.L., Czamanske, G.K., Fedorenko, V.A., Arndt, N.T., Chauvel, C., Bouse, R.M., King, B.-S.W., Knight, R.J. and Siems, D.F., 1993. Isotopic and trace-element constraints on

mantle and crustal contributions to the Siberian continental flood basalts, Noril'sk area, Siberia. Geochim. Cosmochim. Acta, 57: 3677–3704.

Yaroshevsky, A.A., Strizhov, V.P. and Suhoverhov, V.F., 1980. Oxygen isotopic composition in rock-forming minerals of Yoko-Dovyren dunite–troctolite–gabbro–norite massif, North Baikal region. 8th All-Union Symp. on Stable Isotope Geochemistry, Moscow, pp. 56–58 (abstract, in Russian).

Yaroshevsky, A.A., Mironov, Y.V., Ionov, D.A., Abramov, A.V., Krivopliasov, G.S., Koptev-Dvornikov, E.V. and Barmina, G.S., 1983. Internal structure of the Ioko-Dovyren dunite–troctolite–gabbro–norite massif. In: Magmatism and Metamorphism of the BAM Area. Nauka, Novosibirsk, pp. 161–168 (in Russian).

Zartman, R.E. and Haines, S.M., 1988. The plumbotectonic model for Pb isotopic systematics among major terrestrial reservoirs — a case for bi-directional transport. Geochim. Cosmochim. Acta, 52: 1327–1339.

Zindler, A. and Hart, S.R., 1986. Chemical geodynamics. Annu. Rev. Earth Planet. Sci., 14: 493–571.

Zindler, A., Hart, S.R. and Brooks, C., 1981. The Shabogamo Intrusive Suite, Labrador: Sr and Nd isotopic evidence for contaminated mafic magmas in the Proterozoic. Earth Planet. Sci. Lett., 54: 217–235.